A novel nonpeptidyl human c-Mpl activator stimulates human megakaryopoiesis and thrombopoiesis

Takanori Nakamura, Yoshitaka Miyakawa, Atsushi Miyamura, Akiko Yamane, Hidenori Suzuki, Mamoru Ito, Yasuyuki Ohnishi, Norihisa Ishiwata, Yasuo Ikeda, and Nobutomo Tsuruzoe

NIP-004 is a novel synthetic compound developed to display human thrombopoietin (TPO) receptor (c-Mpl) agonist activity. NIP-004 displays species specificity, stimulating proliferation or differentiation of human c-Mpl–expressing cells such as UT-7/TPO and human CD34$^+$ cells but not murine c-Mpl–expressing cells or cynomolgus monkey cells. To test the mechanism of its action, we constructed mutant forms of c-Mpl; murine c-Mpl^{L490H} displayed a response to NIP-004, whereas human c-Mpl^{H499L} lost this response, indicating that histidine in the transmembrane domain of c-Mpl is essential for its activity. Because histidine is not present in the c-Mpl transmembrane domain of rats, hamsters, rhesus macaques, and cynomolgus monkeys, we examined the in vivo efficacy of NIP-004 using mice that received xenotransplants. In immunodeficient nonobese diabetic (NOD)/Shi-*scid*, IL-2Rγ^{null} (NOG) mice receiving transplants of umbilical cord blood–derived CD34$^+$ cells, NIP-004 increased human megakaryoblasts, mature megakaryocytes, and circulating human platelets 6-fold, the latter being morphologically and functionally indistinguishable from normal human platelets. These observations indicate that NIP-004 is a novel human c-Mpl activator and induces human thrombopoiesis. (Blood. 2006;107: 4300-4307)

Introduction

Platelets are important cells for preventing bleeding following injury. Thrombopoietin (TPO), a cytokine produced primarily by the liver and kidney, regulates platelet production by stimulating proliferation and differentiation of hematopoietic stem cells, megakaryocytic progenitor cells, and megakaryocytes via activation of its receptor, c-Mpl.[1-5] c-Mpl belongs to the type I cytokine receptor family, and like erythropoietin (EPO) and granulocyte colony-stimulating factor (GCSF) receptors, a major conformational change of the homodimeric receptor ensues upon TPO binding, followed by phosphorylation of the intracellular domain of c-Mpl and various secondary signaling molecules.[6] Among the signaling molecules activated by TPO are Janus kinases (Jaks) and signal transducers and activators of transcription (STATs), phosphatidylinositol-3-kinase (PI3K)/Akt, and Ras/mitogen-activated protein kinase (MAPK). Activation of these signaling pathways results in the induction of megakaryopoiesis and thrombopoiesis from hematopoietic stem cells.[6] Recombinant human (rh)TPO has been proven to be effective for the treatment of thrombocytopenia in some clinical settings.[7] However, adverse events of therapy have been reported, such as the development of neutralizing antibodies to TPO, followed by thrombocytopenia or pancytopenia.[8] A nonpeptidyl synthetic compound displaying c-Mpl agonistic activity would therefore offer important medical advantages for the treatment of thrombocytopenia.

Toward this end, we developed a novel human c-Mpl (HuMpl) agonist, NIP-004, that displays species specificity. While NIP-004 stimulated HuMpl-expressing cells such as human bone marrow (BM)–, peripheral blood (PB)–, and umbilical cord blood (CB)–derived CD34$^+$ cells, it did not induce proliferation of murine c-Mpl (MuMpl)–expressing cells or colony formation of megakaryocytes with BM cells from murine or cynomolgus monkey. Using mutants of the c-Mpl receptor, we also found that substitution of histidine (His) for leucine (Leu) (L490H) in the MuMpl transmembrane domain allowed the murine receptor to respond to NIP-004. Conversely, HuMpl^{H499L} lost its response to NIP-004, indicating that the His residue is essential for NIP-004 activity. Because this His residue is only present in the HuMpl transmembrane domain, this observation also helps to explain the species specificity of NIP-004. Moreover, this property requires a xenotransplantation model to evaluate the in vivo biologic activities of NIP-004. We used immunodeficient nonobese diabetic (NOD)/Shi-*scid*, IL-2Rγ^{null} (NOG) mice as recipients. These mice exhibit highly potent reconstitutive activity for human hematopoietic stem cells and can maintain human hematopoiesis,[9] including megakaryopoiesis and thrombopoiesis, for at least 6 months after transplantation (Y.M.,

From the Pharmaceutical Research Department, Biological Research Laboratories, Nissan Chemical Industries, Saitama; Department of Internal Medicine, Keio University School of Medicine, Tokyo; Medical Research & Development Center, Tokyo Metropolitan Institute of Medical Science, Tokyo; and Central Institute for Experimental Animals, Kanagawa, Japan.

Submitted November 10, 2005; accepted January 21, 2006. Prepublished online as *Blood* First Edition Paper, February 16, 2006; DOI 10.1182/blood-2005-11-4433.

Several of the authors (T.N., A.M., N.I., and N.T.) are employed by a company (Nissan Chemical Industries) whose product was studied in the present work.

T.N., Y.M., and N.I. designed the study; T.N., A.M., A.Y., and H.S. carried out the research; M.I. and Y.O. contributed live mice; T.N., Y.M., A.M., and H.S. analyzed the data; N.I., Y.I., and N.T. controlled the data; T.N. and Y.M. wrote the paper; and all authors checked the final version of the manuscript.

Reprints: Takanori Nakamura, Pharmaceutical Research Department, Biological Research Laboratories, Nissan Chemical Industries, Ltd, 1470 Shiraoka, Saitama 349-0294, Japan; e-mail: tnakamura@nissanchem.co.jp.

The publication costs of this article were defrayed in part by page charge payment. Therefore, and solely to indicate this fact, this article is hereby marked "advertisement" in accordance with 18 U.S.C. section 1734.

T.N., Hiroshi Yoshida, M.I., Y.O., and Y.I., manuscript in preparation). Using this model, we demonstrated that NIP-004 possesses HuMpl agonistic activity in vivo, and these data support the in vitro activity of the molecule.

Materials and methods

Reagents

Our search for c-Mpl activators was based on proliferation assays using TPO-responsive cell lines with our chemical library (Nissan Chemical Industries, Chiba, Japan), which comprises approximately 50 000 compounds. This process resulted in the identification of several compounds displaying growth-promoting activities. Lead optimization was performed based on the conversion of scaffold and functional groups to increase the growth-promoting activity of the lead compound. Finally, a novel nonpeptidyl HuMpl activator, NIP-004 (5-[(2-{1-[5-(3,4-dichlorophenyl)-4-hydroxy-3-thienyl]ethylidene}hydrazino)carbonyl]-2-thiophenecarboxylic acid) was chemically constructed at Nissan Chemical Industries. We also synthesized another human TPO mimetic, SB-497115. Its structure was presented in a poster presentation at the 46th annual meeting of the American Society of Hematology.[10] Cytokines including rhTPO (PeproTech, Rocky Hill, NJ, and R&D Systems, Minneapolis, MN), rhEPO (Chugai Pharmaceutical, Tokyo, Japan), recombinant murine (rm) interleukin-3 (IL-3) (R&D Systems), rhIL-3 (R&D Systems), and rhGCSF (PeproTech) were obtained as indicated.

Cells

Cells used in this study were human myeloblastic leukemia cell lines UT-7, UT-7/TPO, and UT-7/EPO (kindly donated by Dr Norio Komatsu, University of Yamanashi, Japan), murine pro–B-cell line Ba/F3 (Riken Cell Bank, Tsukuba, Japan), and human embryonic kidney cell line HEK293 (Health Science Research Resources Bank, Osaka, Japan). UT-7/EPO-HuMpl in which the human *c-mpl* gene was genetically introduced under the control of cytomegalovirus (CMV) promoter was kindly donated by Dr Norio Komatsu. Stable transfectants such as UT-7/EPO-MuMpl, Ba/F3-HuMpl, Ba/F3-MuMpl, and Ba/F3-HuGCSFR were established to transfect human or murine *c-mpl* or human *gcsfr* genes under the control of the CMV promoter (pcDNA3 vector; Invitrogen, Carlsbad, CA) using electroporation. UT-7 cells and the variant cell lines were maintained in Iscove modified Dulbecco medium (IMDM) supplemented with 10% fetal bovine serum (FBS) and rhIL-3, rhTPO, or rhEPO. Ba/F3 cells and their transfectants were maintained in RPMI 1640 medium supplemented with 10% FBS and rmIL-3, rhTPO, or rhGCSF. HEK293 cells were cultured in Dulbecco modified Eagle medium (DMEM) containing 10% FBS. Human primary hematopoietic progenitor cells were BM-, PB-, or CB-derived $CD34^+$ cells (Cambrex, East Rutherford, NJ). Cynomolgus BM-derived $CD34^+$ cells were prepared from BM mononuclear cells (Cambrex) using a CD34 progenitor cell selection system (Dynabeads M-450 CD34; Dynal Biotech, Oslo, Norway). Murine BM cells were prepared from BALB/c mice (Japan SLC, Shizuoka, Japan).

Genes

The cDNAs of human or murine *c-mpl* or human *gcsfr* were amplified by reverse transcriptase–polymerase chain reaction (RT-PCR) using a SuperScript First-Strand Synthesis System (Invitrogen) and each specific primer set as follows: human *c-mpl* primer set (sense, 5′-ATGCCCTCCTGGGCCCTCTT-3′; antisense, 5′-TCAAGGCTGCTGCCAATAGCT-3′), murine *c-mpl* primer set (sense, 5′-ATGCCCTCTTGGGGCCCTCTTCAT-3′; antisense, 5′-TCAGGGCTGCTGCCAAIAGCTTAGT-3′), and human *gcsfr* primer set (sense, 5′-ATGGCAAGGCTGGGAAACTGCA-3′; antisense, 5′-CTAGAAGCTCCCCAGCGCCTCCA-3′). Full-length cDNAs were cloned into pCR vector (Invitrogen) and were subcloned into the *Eco*RI site of the pcDNA3 vector. In vitro mutagenesis of human or murine *c-mpl* genes ($HuMpl^{1\text{-}504}$ or $MuMpl^{1\text{-}491}$) was performed using QuikChange Site-Directed Mutagenesis Kit (Stratagene, La Jolla, CA) and a specific primer set as follows: $HuMpl^{1\text{-}504}$ primer set (sense, 5′-GGTGACCGCTCTGCTACTAGTGCTGGGCC-3′; antisense, 5′-GGCCCAGCACTAGTAGCAGAGCGGTCACC-3′) and $MuMpl^{1\text{-}491}$ primer set (sense, 5′-GTGACTGCTCTGCACCTGGTGCTGAGC-3′; antisense, 5′-GCTCAGCACCAGGTGCAGAGCAGTCAC-3′), according to the protocols of the manufacturer. The cDNAs of cynomolgus monkey, rhesus macaque, common marmoset, and squirrel monkey *c-mpl* homologous genes were amplified by RT-PCR using a human *c-mpl* primer set and total RNA isolated from whole blood for each nonhuman primate (Hamri, Ibaraki, Japan). A human *c-mpl* primer set and a nested primer set (sense, 5′-CTTTGGAACCCGATACGTGTG-3′; antisense, 5′-GGAGGATTTCCAGGAGGCTG-3′), designed for high-sequence homology between human and murine *c-mpl* genes, were used for amplification in Japanese white rabbit (Kitayama Labes, Nagano, Japan), Syrian hamster, Hartley guinea pig (Japan SLC), and Wistar rat (Charles River Japan, Kanagawa, Japan) *c-mpl* homologous genes. The cDNAs of these animal *c-mpl* homologous genes were cloned into the pCR vector, and their sequences were identified as accession numbers AB235193, AB235192, AB235194, AB235195, AB235199, AB235198, AB235196, and AB235197 for cynomolgus monkey, rhesus macaque, common marmoset, squirrel monkey, Japanese white rabbit, Syrian hamster, Hartley guinea pig, and Wistar rat, respectively.

Proliferation assay

A total of 2×10^3 to 6×10^3 cells were harvested in IMDM or RPMI 1640 medium containing 10% FBS and cytokines or NIP-004 at the indicated final concentration and incubated in a CO_2 incubator (5% CO_2, 37°C) for 3 to 4 days, depending on the cell line. Cell proliferation was assayed using WST-8 reagent (Kishida Chemical, Osaka, Japan) according to instructions from the manufacturer. The formazan pigment was detected by measuring absorbance at 450 nm with a 96-well microplate reader, Spectramax 190 (Molecular Devices, Sunnyvale, CA) or Model 550 (Bio-Rad, Hercules, CA).

Immunoprecipitation and Western blotting

A total of 2×10^7 UT-7/EPO-HuMpl cells were starved for 17 hours at 37°C and stimulated with 20 μg/mL NIP-004 or 30 ng/mL hTPO at 37°C for 15 minutes. Cells were solubilized in 1 mL TNE buffer comprising 20 mM Tris-HCl buffer (pH 7.4), 150 mM NaCl, 1 mM ethylenediaminetetraacetic acid (EDTA), 1% Triton X-100, 1 mM phenyl methane sulfonyl fluoride, 1 mM Na_3VO_4, and 1:400-diluted protease inhibitor cocktail (Sigma, St Louis, MO). After centrifugation, cleared lysates were incubated with anti-Mpl (IBL, Gunma, Japan), anti-Jak2 (Upstate Biotechnology, Waltham, MA), and anti-STAT5a (Upstate Biotechnology) for 1 hour at 4°C. Immune complexes adsorbed with protein G–Sepharose were resolved by 7.5% sodium dodecyl sulfate–polyacrylamide gel electrophoresis. Transferred polyvinylidene fluoride membrane (Millipore, Bedford, MA) was immunoblotted with monoclonal antiphosphotyrosine antibody (BD PharMingen, San Diego, CA) or anti-Mpl, anti-Jak2, or anti-STAT5a and alkaline phosphatase (AP)–labeled secondary antibody (Invitrogen); then the proteins were visualized using nitroblue tetrazolium and 5-bromo-4-chloro-3-indolyl phosphate reagents (Bio-Rad).

Megakaryocyte colony-forming unit assay

Megakaryocyte colony-forming unit (CFU-MK) assays were performed using MegaCult-C (StemCell, Vancouver, BC, Canada) according to the manufacturer's protocol. A total of 7.5×10^3 human or cynomolgus monkey BM-derived $CD34^+$ cells or 2.5×10^3 human CB- or PB-derived $CD34^+$ cells were cultured with NIP-004 or rhTPO for 11 days in collagen-based, semisolid medium. After fixation, megakaryocytes were visualized with antibody against CD41a using AP staining. Nuclei were stained with Evans blue. Stained colonies were examined under a Nikon Eclipse E800 microscope equipped with a 10 × 0.3 numeric aperture (NA) objective lens (Nikon, Tokyo, Japan). Images were captured using an Olympus Camedia C300 digital camera (Olympus, Tokyo, Japan). The murine CFU-MK assay was performed as follows: 3×10^5 murine BM cells were cultured with NIP-004 or rhTPO for 7 days in agar-based, semisolid medium comprising IMDM, 1% bovine

serum albumin, 0.6 mg/mL transferrin, 8 μg/mL cholesterol, and 0.1% agar. After fixation in glutaraldehyde, megakaryocytes were visualized by measuring the internal acetyl cholinesterase activity as previously described.[11]

Luciferase assay

HEK293 cells were transfected with pcDNA-HuMpl, HuMpl$^{\Delta 504}$, MuMpl, or MuMpl$^{\Delta 496}$ in combination with pXM-MGF (STAT5) and acute phase response element–luciferase construct (kindly donated by Dr Akihiko Yoshimura[12]) using the Effectene transfection reagent (Qiagen, Hilden, Germany). Twenty-four hours after transfection, cells were starved for 8 hours, followed by stimulation with rhTPO or NIP-004 at the indicated concentration for 18 hours. Cell extracts were prepared, and luciferase activity was measured using PicaGene reagent (Toyo B-NET, Tokyo, Japan) according to the manufacturer's instructions.

Xenotransplantation assay

NOG mice were developed at the Central Institute for Experimental Animals (Kanagawa, Japan) and were maintained under specific pathogen-free conditions. Shortly before cell transfer, 8- to 10-week-old NOG mice were irradiated with 2.4 Gy x-rays. Frozen 1×10^5 CB-derived CD34$^+$ cells were washed with IMDM medium supplemented with 0.1% BSA and the cells then intravenously inoculated into mice. After transplantation, mice were provided with sterile water containing prophylactic neomycin sulfate (Gibco BRL, Grand Island, NY). Mice received daily subcutaneous administration of NIP-004 for the indicated period at a dosage of 10 or 30 mg/kg (with PBS containing 1.6% PEG400 and 2.4% ethanol vehicle) from 2 to 6 months after transplantation. Whole blood containing EDTA-2Na or 0.38% sodium citrate was prepared recurrently from a mouse. Complete blood counts were obtained using a K-4500 automated analyzer (Sysmex, Hyogo, Japan). BM cells were obtained by flushing the femurs, and cell numbers were counted using a hemocytometer (Erma, Tokyo, Japan) after staining with Turk solution.

Flow cytometry analysis

To detect human cells in murine blood, multicolor flow cytometry was performed using an EPICS-XL flow cytometer (Beckman Coulter, Franklin Lakes, NJ). Samples were incubated with the indicated antibodies for 30 minutes at 4°C and were depleted of erythrocytes by fixation in fluorescence-activated cell sorter (FACS) lysing solution (BD PharMingen). Antibodies used in this study were as follows: anti–human CD33–fluorescein isothiocyanate (FITC), CD3-FITC, CD41a-FITC, CD34-FITC, CD71-FITC, CD34-phycoerythrin (PE), CD41a-PE, CD19-PE, CD45-PE Texas red (ECD), CD38-PE 5-succinimidylester (PC5), anti–murine CD45-FITC, and CD41-FITC. Antibodies conjugated with FITC, PE, or PC5 were purchased from BD PharMingen. Antibodies conjugated with ECD were purchased from Immunotech (Marseilles, France). Platelets were incubated with the indicated antibodies at room temperature and directly applied to the flow cytometer. Human platelets were examined by double staining with anti–murine CD41-FITC antibody and anti–human CD41a-PE antibody, in which platelets were identified by size and gated by forward and side scatter. The actual number of human CD41a$^+$ platelets was calculated as follows: actual human CD41a$^+$ platelet count = (human CD41a$^+$ platelet count/[human CD41a$^+$ platelet count + murine CD41$^+$ platelet count]) × whole platelet count.

To detect human megakaryocyte ploidy, BM cells from NOG mice that received xenotransplants were stained using anti–human CD41a-PE antibody and fixed with 1% paraformaldehyde. Fixed cells were stained using 7-amino-actinomycin D (7-AAD) dye (Immunotech) and examined by 2-color cytometric analysis.

Immunohistochemistry

Femurs of NOG mice that received xenotransplants were removed for histological examination. Tissue was fixed in neutral buffered formalin and decalcified, followed by paraffin embedding and sectioning. Immunohistochemistry was performed with murine monoclonal antibodies against human CD42b (Chemicon, Temecula, CA) and EnVision+ peroxidase staining kit (Dako, Carpinteria, CA). Stained sections were examined using an Olympus BX51 microscope equipped with a 10 × 0.3 NA objective and connected to an Olympus DP12 camera, using DP12 software.

Electron microscopic analysis of human platelets from mice undergoing xenotransplantation

Immunoelectron microscopy was performed as previously described.[13] Whole blood containing 0.38% sodium citrate, 1 μM prostaglandin E_1, 2 U/mL apyrase, and 2 mM aspirin (Sigma) was prepared. Platelet-rich plasma (PRP) was fixed with glutaraldehyde and sequentially immersed in 1 M sucrose, 1.84 M sucrose, and 1.84 M sucrose with 20% polyvinylpyrrolidone (MW 10 000; Sigma) in PBS. After freezing platelets in liquid nitrogen, ultrathin frozen sections were cut using an Ultracut ultramicrotome (Reichert, Vienna, Austria) with a cryoattachment (FC-4E; Reichert) at −90°C. Sections were mounted on nickel grids and incubated with anti–human CD41a monoclonal antibody (Immunotech), followed by goat anti–mouse IgG coupled to colloidal gold (10 nm; Amersham, Olen, Belgium). Sections were stained with uranyl acetate and subjected to adsorption staining using a mixture of polyvinyl alcohol and uranyl acetate. Stained sections were examined using a JEM 1200EX electron microscope (JEOL, Tokyo, Japan) at an accelerating voltage of 80 kV.

Functional studies of platelets from NOG mice undergoing xenotransplantation

Functional studies of platelets were performed as previously described.[14] After administration of NIP-004 (30 mg/kg/d subcutaneously for 14 days) or vehicle, PRP was obtained, and *N*-2-hydroxyethylpiperazine-*N*′-2-ethanesulfonic acid (HEPES)–Tyrode buffer (138 mM NaCl, 0.42 mM NaH_2PO_4, 2.68 mM KCl, 12 mM $NaHCO_3$, 10 mM HEPES, 5 mM glucose, and 1.7 mM $MgCl_2$, pH 7.4) was added at a 1:9 ratio. To determine the expression of P selectin upon agonist stimulation, platelets were stimulated using 10 μM ADP or vehicle for 15 minutes in the buffer containing anti–human CD62p-PE antibody (BD PharMingen). After fixation with 0.5% paraformaldehyde, cells were washed and incubated with anti–human CD41a-PC5 (BD PharMingen) and anti–murine CD41-FITC antibody. To determine the activation of GPIIb-IIIa, platelets were stimulated with 0 to 10 μM ADP for 15 minutes with PAC-1–FITC (BD Pharmingen), anti–human CD42b-PC5, and anti–murine CD61-PE antibody and then fixed and washed. Stained platelets were analyzed by flow cytometry.

Statistical analysis and ethical considerations

Results are expressed as mean ± SD or mean ± SEM as indicated. Differences between groups were examined for statistical significance using the Student *t* test. Animal experiments were conducted according to the "Guideline for animal experimentation"[15] by the Japanese Association for Laboratory Animal Science. All experimental protocols were approved by the ethics review committees for animal experimentation of Keio University and Nissan Chemical Industries.

Results

NIP-004 is a novel human c-Mpl activator

We conducted a search for c-Mpl activators based on proliferation assays with TPO-responsive UT-7/TPO and UT-7/TPO-HuMpl cell lines. Screened agents were obtained from our chemical library, comprising approximately 50 000 compounds. This process resulted in the identification of several compounds displaying growth-promoting activity. Lead optimization was subsequently performed to create c-Mpl activators with greater growth-promoting activity. NIP-004 is a synthetic compound (MW 455; Figure 1A) and stimulated the proliferation of UT-7/TPO,[16] a human leukemia cell line endogenously expressing HuMpl, in a

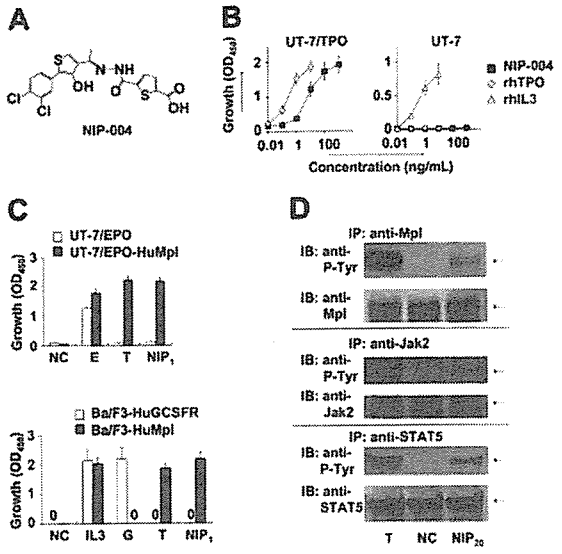

Figure 1. NIP-004 is a novel human c-Mpl activator. (A) Chemical structure of NIP-004. (B) Dose-dependent proliferation of UT-7/TPO cells, but not parental UT-7 cells, by NIP-004. Recombinant human TPO and rhIL-3 induced proliferation of UT-7/TPO and parental UT-7 cells, respectively. (C) TPO and NIP-004 induced proliferation of UT-7/EPO-HuMpl but not UT-7/EPO (top panel). EPO stimulated proliferation of UT-7/EPO and UT-7/EPO-HuMpl as a positive control. NIP-004 stimulated proliferation of Ba/F3-HuMpl but not Ba/F3-HuGCSFR (bottom panel). GCSF stimulated Ba/F3-HuGCSFR cells. TPO induced proliferation of Ba/F3-HuMpl cells as a positive control. IL-3 stimulated both Ba/F3-HuGCSFR and Ba/F3-HuMpl. Data in panels B-C are expressed as the mean ± SEM (n = 3 to 4) or mean ± SD (n = 2; Ba/F3-HuGCSFR) from independent duplicate experiments. (D) Induction of tyrosine phosphorylation of c-Mpl, Jak2, and STAT5 in UT-7/EPO-HuMpl cells by TPO and NIP-004. NC indicates negative control; E, 0.1 U/mL rhEPO; IL-3, 0.1 ng/mL rmIL-3; G, 10 ng/mL rhGCSF; T, 10 ng/mL rhTPO; NIP_1, 1 μg/mL NIP-004; NIP_{20}, 20 μg/mL NIP-004; P-Tyr, phosphotyrosine.

dose-dependent manner (Figure 1B). Compared with 10 ng/mL rhTPO, which induces a maximal response in this cell line, the median effective concentration (EC_{50}) of NIP-004 was 23 ng/mL (50 nM) in UT-7/TPO cells (Figure 1B). Proliferation of UT-7 cells, the parental cell line of UT-7/TPO, can be induced by cytokines such as human IL-3, human granulocyte-macrophage colony-stimulating factor (GMCSF), IL-6, stem cell factor, and EPO but not by TPO because UT-7 does not display c-Mpl.[16,17] Consistent with its action through c-Mpl, NIP-004 did not induce the growth of UT-7 cells (Figure 1B, right panel). Recombinant human IL-3 induced proliferation of UT-7 cells as a positive control. We also confirmed the roles of HuMpl using other cell lines as follows. When HuMpl was introduced into UT-7/EPO cells,[18,19] UT-7/EPO-HuMpl transfectants responded to both rhTPO and NIP-004 (Figure 1C, upper panel). NIP-004 induced proliferation of Ba/F3-HuMpl cells but not Ba/F3-HuGCSFR cells expressing human GCSF receptor, indicating that NIP-004 acts on c-Mpl (Figure 1C, lower panel). Recombinant human GCSF and rhTPO stimulated proliferation of Ba/F3-HuGCSFR and Ba/F3-HuMpl cells as positive controls, respectively (Figure 1C).

A large body of evidence indicates that like other type I family cytokine receptors, TPO signaling is dependent on Jak-induced phosphorylation of tyrosine residues within the cytoplasmic domain of c-Mpl. Subsequently, secondary signaling molecules, including STAT5, are recruited to the phosphotyrosine residues and are activated by their phosphorylation.[6] Administration of 20 μg/mL NIP-004 induced phosphorylation of c-Mpl, Jak2, and STAT5 proteins in UT-7/EPO-HuMpl cells after 15 minutes (Figure 1D). TPO was used as positive control stimulation (Figure 1D). In addition, rhTPO and NIP-004 induced phosphorylation of Akt, an antiapoptotic protein in the PI3K-Akt signaling pathway, via c-Mpl (data not shown).

We next examined whether NIP-004 possessed the capacity to induce megakaryocyte differentiation using colony-forming assays and histologic staining with a monoclonal antibody against integrin GPIIb-IIIa (CD41a), a specific marker of the megakaryocyte-platelet lineage.[20] NIP-004 1 μg/mL alone stimulated colony formation of CD41a+ megakaryocytes from human BM-derived $CD34^+$ hematopoietic progenitor cells in serumfree, semisolid cultures (Figure 2A). NIP-004 induced maturation of megakaryocytes, since large polyploid CD41a+ cells appeared in the colony (Figure 2A). NIP-004 increased the number of CFU-MKs from human BM-derived $CD34^+$ cells in a dose-dependent manner (Figure 2B, left panel). Furthermore, a number of CFU-MKs developed from human CB- or PB-derived $CD34^+$ cells treated with NIP-004 (Figure 2B). The efficiency of CFU-MK production in $CD34^+$ cells was higher in CB- and PB-derived cells than in BM-derived cells, as previously reported (Figure 2B, right panel).[21]

NIP-004 displays species-specific activity

Because NIP-004 was obtained using cells expressing HuMpl, the effects of NIP-004 on c-Mpl from other species were examined. NIP-004 did not induce proliferation of UT-7/EPO-MuMpl or Ba/F3-MuMpl cells, which were engineered to express murine c-Mpl receptor (Figure 3A). Furthermore, NIP-004 did not increase the number of CFU-MK colonies from murine BM cells or cynomolgus monkey BM-derived $CD34^+$ cells within the effective dosage for human cells (Figure 3B). Likewise, rhesus macaque BM-derived $CD34^+$ cells failed to form CFU-MK colonies in the presence of a NIP-004–derived compound (data not shown). These results indicate that NIP-004 displays species specificity.

To identify the molecular basis for the species specificity displayed by NIP-004, we analyzed the amino acid sequence of c-Mpl from 2 nonhuman primates, cynomolgus and rhesus monkeys, and compared them with the HuMpl and MuMpl. Cynomolgus c-Mpl displayed the highest level of sequence homology, 96%

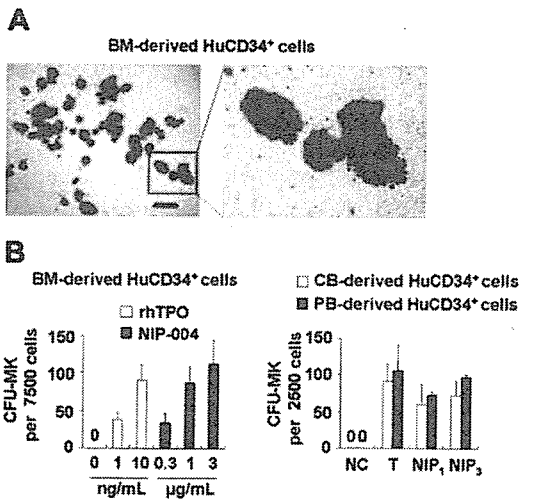

Figure 2. Stimulation of megakaryocyte colony formation from human $CD34^+$ cells by NIP-004. (A) Morphology of CFU-MK colonies obtained from human BM-derived $CD34^+$ cells treated with 1 μg/mL NIP-004. CFU-MKs were visualized with AP-labeled antibody against human CD41. Polyploid megakaryocytes are shown in detail in the right panel. Bar, 200 μm. (B) The number of CFU-MKs from human BM-, CB-, and PB-derived $CD34^+$ cells treated with 1 to 3 μg/mL NIP-004 was similar to that with 10 ng/mL rhTPO. Results are expressed as mean ± SEM from 4 independent experiments (BM) or mean ± SD from 2 independent experiments (CB and PB). NC indicates negative control; T, 10 ng/mL rhTPO; NIP_1, 1 μg/mL NIP-004; NIP_3, 3 μg/mL NIP-004.

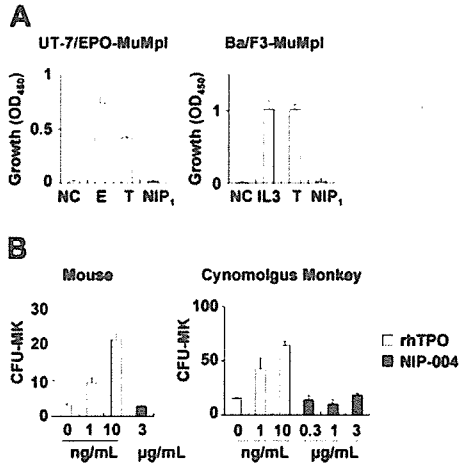

Figure 3. NIP-004 displays species-specific activity. (A) NIP-004 failed to stimulate proliferation of UT-7/EPO-MuMpl– and Ba/F3-MuMpl–expressing murine Mpl. In contrast, EPO and TPO stimulated induced proliferation of UT-7/EPO-MuMpl as a positive control. IL-3 and TPO enhanced proliferation of Ba/F3-MuMpl as a positive control. Data are expressed as the mean ± SEM from 3 independent experiments. (B) Recombinant human TPO stimulated CFU-MK colony formation from murine and cynomolgus monkey–derived bone marrow cells in a dose-dependent manner. In contrast, NIP-004 failed to induce CFU-MK colonies under the same conditions. Data are expressed as the mean ± SD of duplicate assays. NC indicates negative control; E, 0.1 U/mL rhEPO; IL-3, 0.1 ng/mL rmIL-3; T, 10 ng/mL rhTPO; NIP_1, 1 µg/mL NIP-004.

identical to HuMpl, with only 22 amino acids differing between the 2 species, and 12 of the 22 amino acids of HuMpl differed from rhesus c-Mpl. Comparison of these 12 amino acid residues as either hydrophobic or hydrophilic, and either electrically charged or uncharged, revealed distinguishing features of the amino acid residues. His at position 499 from the N-terminal end in the transmembrane domain of HuMpl is specific for humans. We thus performed site-directed mutagenesis for this residue in HuMpl and MuMpl (Figure 4A) and analyzed STAT5 activation via each receptor in the HEK293 cell line using the STAT-reporter gene assay (Figure 4B). Wild-type HuMpl, but not MuMpl, activated STAT5 after stimulation with NIP-004 in a dose-dependent manner. HuMpl with His499 mutated to Leu failed to induce STAT5 activation following stimulation with NIP-004, although rhTPO was active. Conversely, when MuMpl was engineered to contain His490, as is present in the human receptor, it was then capable of activating STAT5 (Figure 4B). These observations indicate that His in the transmembrane domain of c-Mpl is essential for NIP-004 to function as a c-Mpl activator. We therefore assessed the c-Mpl amino acid sequence in several common experimental animals to find a suitable species in which we could evaluate the in vivo efficacy of NIP-004 for platelet production. Our search revealed no animals with His in the transmembrane domain of c-Mpl among the common marmoset, squirrel monkey, Japanese white rabbit, Syrian hamster, Hartley guinea pig, and Wistar rat (Figure 4C).

NIP-004 stimulates human megakaryopoiesis in NOG mice undergoing xenotransplantation

Because we were unable to find suitable experimental animals with His in the c-Mpl transmembrane domain to evaluate the effects of NIP-004, we selected a xenotransplantation model to examine in vivo efficacy of the compound for human megakaryopoiesis and thrombopoiesis. We used NOG mice to develop this new experimental animal model of human megakaryopoiesis, because this species displayed high potency for reconstituting human hematopoietic progenitor cells.[9]

In NOG mice receiving transplants with human CB-derived $CD34^+$ cells, treatment with 30 mg/kg/d NIP-004 for 2 weeks resulted in a 3-fold increase in human (Hu) $CD41a^+$ megakaryocytes in murine BM (0.9% in NIP-004–treated mice versus 0.3% in vehicle-treated mice) but no alteration in the number of murine $CD41^+$ megakaryocytes (Figure 5A). This dosage of NIP-004 achieved a plasma concentration of approximately 0.6 µg/mL at steady state. NIP-004 thus enhanced human megakaryopoiesis at an in vivo dosage comparable to that in the in vitro colony formation study (Figure 2B).

NIP-004 did not influence the total number of nucleated cells, the percentage of human or murine $CD45^+$ leukocytes, the percentage of $HuCD38^+CD19^+$ B lymphoid or $HuCD38^{low/-}CD33^+$ myeloid cells in $HuCD45^+$ cells, or the number of $HuCD45^-CD71^+$ erythroblasts in murine BM (Figure 5B). Although the total percentage of $HuCD45^+CD34^+$ hematopoietic progenitor cells was not altered by NIP-004 administration, we observed a 1.5-fold increase in the percentage of $HuCD45^+CD34^+CD41a^+$ megakaryoblasts (Figure 5C). This finding indicates that NIP-004 enhanced the number of human megakaryoblasts and megakaryocytes in xenotransplanted murine BM.

We next examined whether NIP-004 induced the maturation of megakaryocytes in vivo. DNA ploidy of $HuCD41^+$ megakaryocytes was analyzed by flow cytometry using anti-HuCD41 antibody and 7-AAD dye. In mice that received transplants, BM cells were prepared after treatment with NIP-004 (30 mg/kg/d for 2 weeks) or vehicle. Each ploidy class of human megakaryocytes was increased in mice treated with NIP-004, with statistical significance in all but the 32N class (Figure 5D). NIP-004 increased the percentage of $HuCD41a^+$ 128N megakaryocytes by a mean 2.7 ± 0.1 times.

Similar results were obtained in immunohistochemistry. BM from mice receiving xenotransplants was stained with monoclonal antibodies against human integrin GPIb (HuCD42b) to specifically visualize human megakaryocytes (Figure 5E-F). Murine megakaryocytes were not stained with this antibody. NIP-004 (30 mg/kg/d for

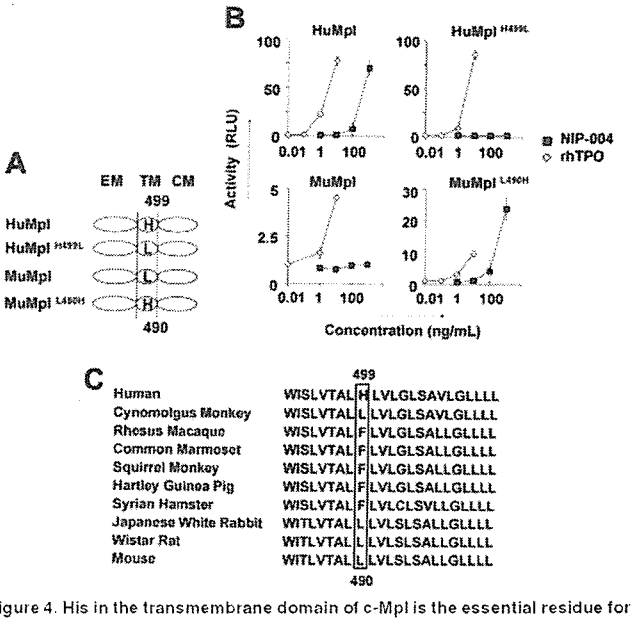

Figure 4. His in the transmembrane domain of c-Mpl is the essential residue for NIP-004. (A) Schema of site directed mutagenesis in HuMpl and MuMpl. EM indicates extracellular module; TM, transmembrane module; CM, cytoplasmic module. (B) STAT5-reporter gene assay showing induction of STAT activation via HuMpl and $MuMpl^{L490H}$ but not $HuMpl^{H499L}$ or MuMpl following NIP-004 administration. Data are expressed as the mean ± SD from 2 independent experiments. (C) Comparison of amino acid sequences of c-Mpl transmembrane domain from various animals. His499 only exists in humans and not in other species.

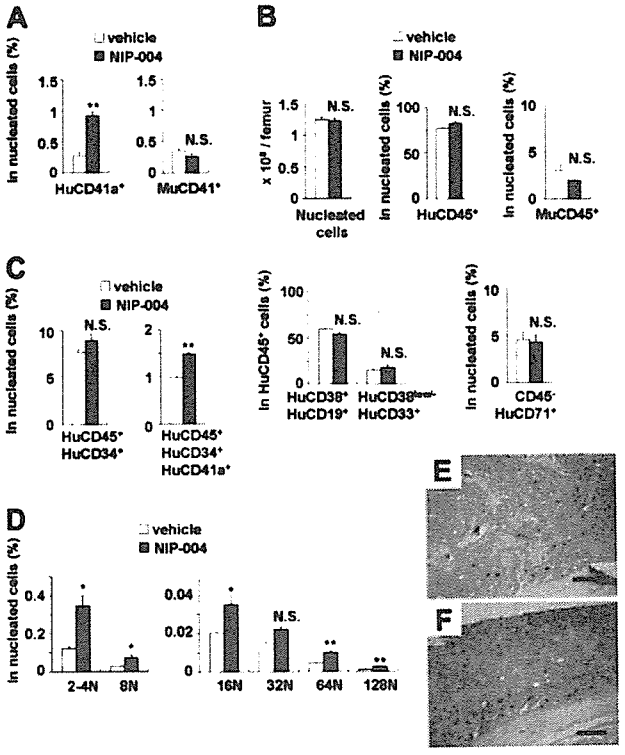

Figure 5. Effects of NIP-004 on human megakaryopoiesis in xenotransplanted murine bone marrow. (A) NIP-004 increased HuCD41a$^+$ megakaryocytes, but not MuCD41$^+$ megakaryocytes, in NOG mice receiving xenotransplants. (B) NIP-004 had no significant effect on the number of total nucleated cells and the percentage of other cell lines in murine BM. (C) NIP-004 increased the number of human megakaryocytic progenitor cells (HuCD45$^+$CD34$^+$CD41a$^+$) but not HuCD45$^+$CD34$^+$ hematopoietic progenitor cells. (D) FACS analysis of DNA ploidy of HuCD41$^+$ megakaryocytes. NIP-004 induced maturation of human megakaryocytes in the BM of NOG mice receiving xenotransplants. Data in panels A-D are expressed as mean ± SEM (n = 3). $^*P < .05$, $^{**}P < .01$ between NIP-004 and vehicle. N.S. indicates no significant difference compared with vehicle. Similar results were obtained from 2 independent experiments. (E-F) Immunohistochemical staining of xenotransplanted murine BM with a monoclonal antibody against human integrin GPIb (HuCD42b). Sections were obtained from the femurs of mice treated with vehicle (E) or NIP-004 (F). Bars, 200 μm

2 weeks) clearly enhanced human megakaryopoiesis (Figure 5E-F). These findings demonstrate that NIP-004 specifically enhanced human megakaryopoiesis but not other types of human hematopoiesis in mice receiving xenotransplants.

NIP-004–induced production of human platelets in mice undergoing xenotransplantation

All NOG mice (n = 84) receiving transplants with human hematopoietic cells produced human platelets for at least 1 to 6 months. To clarify whether NIP-004 increased circulating human platelets in mice receiving xenotransplants, several administration protocols were used. NIP-004 30 mg/kg/d subcutaneously for 2 weeks induced a statistically significant 4.4-fold increase in circulating human CD41a$^+$ platelets at day 14 (Figure 6A). NIP-004 did not influence the total number (human and murine) of red blood cells, platelets, and white blood cells (Figure 6B, upper panel). The number of murine CD41$^+$ platelets and chimerisms of HuCD45$^+$ leukocytes was not altered by NIP-004 administration (Figure 6B, middle panel). Furthermore, NIP-004 did not influence the percentage of HuCD19$^+$ B lymphoid, HuCD3$^+$ T lymphoid, or HuCD33$^+$ myeloid cells among the circulating HuCD45$^+$ cells in mice receiving xenotransplants (Figure 6B, lower panel).

Next, the effect of the administration period or dosage was examined. When NOG mice receiving transplants with HuCD34$^+$ cells were treated with NIP-004 30 mg/kg/d for 5 weeks, there was a 6.4-fold increase in human platelets (Figure 6C). In mice receiving transplants, treatment with 10 mg/kg/d NIP-004 for 2 weeks resulted in a 3.2-fold increase in human platelets (Figure 6C). Human platelet counts returned to pretreatment levels after cessation of drug treatment (Figure 6C). When mice were reexposed to NIP-004, the number of human platelets increased again, suggesting human megakaryopoiesis was maintained in NOG mice undergoing xenotransplantation (data not shown).

To elucidate whether the human platelets in NIP-004–treated mice displayed normal morphologic features, immunoelectron microscopic analysis was performed using antibodies against HuCD41 and MuCD41. Platelets were prepared from mice after administration of NIP-004 30 mg/kg/d subcutaneously for 2 weeks, when human platelet chimerism increased from 2% at baseline to approximately 9%. Human platelets were labeled with gold particles to visualize HuCD41 (Figure 7A). Human platelets labeled with gold particles were larger than unlabeled murine platelets. Human platelets exhibited discoid forms similar to normal human peripheral platelets,[13] containing some granules, mitochondria, and other organelles. Conversely, when antibody against MuCD41 was used, some platelets were not labeled with gold particles on the surface (data not shown). These observations indicate that NIP-004 administration in mice receiving xenotransplants resulted in the production of human platelets that were morphologically indistinguishable from normal human platelets.

We next studied whether the circulating human platelets in NOG mice were functional. Platelets were obtained from either NIP-004– or vehicle-treated mice. When platelets were stimulated with 10 μM ADP, surface expression of P selectin (CD62p) was observed on human platelets from NIP-004–treated mice at almost

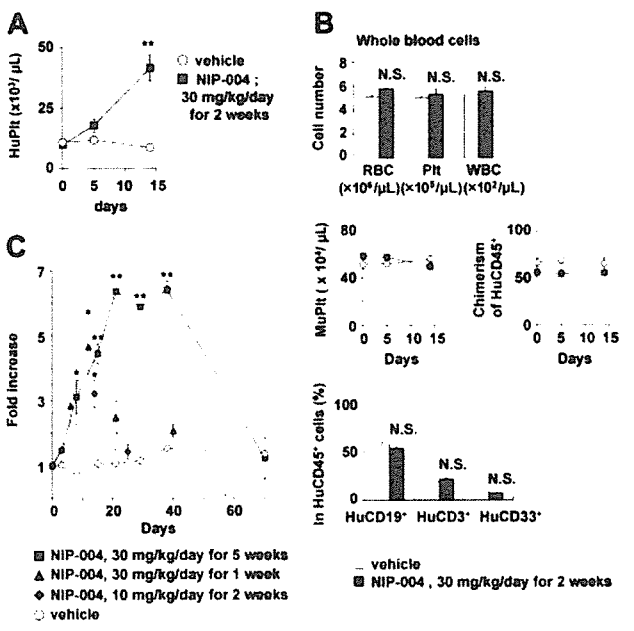

Figure 6. NIP-004–induced production of human platelets in NOG mice receiving xenotransplants. (A) NIP-004 increased the number of circulating human platelets in NOG mice. (B) NIP-004 did not change the number of murine platelets or chimerism of HuCD45$^+$ cells. NIP-004 had no effect on the percentage of human B (CD19$^+$) cells, human T (CD3$^+$) cells, and human myeloid (CD33$^+$) cells in the peripheral HuCD45$^+$ cells. Data from panels A-B are expressed as the mean ± SEM (n = 3). (C) NIP-004 increased the number of circulating human platelets. The increase was calculated as the number of circulating human platelets at individual time points divided by the pretreatment value (day 0). Data are expressed as the mean ± SEM (n = 3 to 6) or mean ± SD (n = 2). $^*P < .05$, $^{**}P < .01$ between NIP-004 and vehicle at individual time points. N.S. indicates no significant differences compared with vehicle.

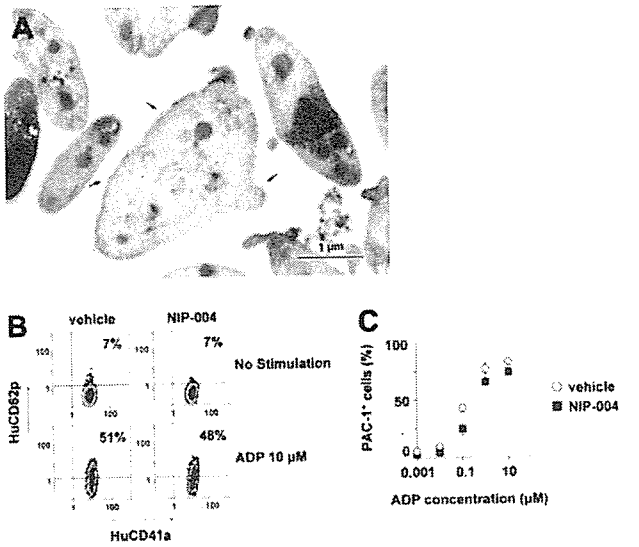

Figure 7. Morphologic and functional features of human platelets induced by NIP-004 in NOG mice. (A) Immunoelectron microscopy using antibody against HuCD41a identified human platelets in PRP derived from NIP-004–treated mice. The surface of a platelet located in the center is labeled with gold particles (arrow), indicating that it is of human origin. Bar, 1 μm. (B) P selectin (HuCD62p) expression upon ADP stimulation in human platelets was similarly increased in both vehicle- and NIP-004–treated mice. (C) After stimulation with various concentrations of ADP, there was a similar dose-dependent escalation in the percentage of PAC-1–positive human platelets from vehicle- and NIP-004–treated NOG mice receiving xenotransplants. PAC-1 antibody specifically recognizes the activated form of GPIIbIIIa. Data are expressed as the mean ± SEM (n = 4).

the same rate as vehicle-treated mice (Figure 7B), suggesting that α-granules were released.[14] In addition, we examined whether the human platelets found in NIP-004–treated mice receiving xenotransplants exhibited a similar response to ADP stimulation as normal platelets (Figure 7C). The active form of fibrinogen receptor (GPIIb-IIIa integrin) on human platelets was recognized by binding of the PAC-1 monoclonal antibody (Figure 7C).[14] Human platelet activation by ADP was dose dependent, and the mean concentration of ADP required to produce 50% activation of the human platelets was 0.6 μM in NIP-004–treated and 0.3 μM in vehicle-treated mice (Figure 7C). These observations indicated that NIP-004 had no adverse effects on the function of human platelets.

Discussion

In this study, we identified a nonpeptidyl synthetic compound, NIP-004, as a novel c-Mpl activator. In vitro studies revealed that rhTPO and NIP-004 display a similar potential to activate HuMpl. However, unlike rhTPO, NIP-004 displays species specificity. Recently, nonpeptidyl small molecule compounds such as benzodiazepine derivatives,[22] hydrazinonaphthalenes and azonaphthalenes,[23,24] and substituted thiazole[25] and xanthocillins[26] have been reported as possessing TPO-like activity. In some cases, c-Mpl agonists such as SB394725 exhibit species specificity.[27] This study confirms that His in the transmembrane domain of c-Mpl is essential for NIP-004 agonist activity (Figure 4B). Although His exists in the transmembrane domain of HuGCSFR and mouse IL-3/GM-CSF/IL-5 common β subunit 2 (Muβc2) (ENSP00000342623 and ENSMUSP00000006263 from the Ensembl database, respectively), Ba/F3-HuGCSFR cells expressing Muβc2 and HuGCSFR did not respond to NIP-004 (Figure 1C). Because the position of His in the transmembrane domains of HuGCSFR and Muβc2 does not correspond to HuMpl, we speculate that the His may need to be present in the middle of a transmembrane domain and/or interact with other amino acids of c-Mpl for NIP-004 agonist activity. It has been reported that the point mutation of Leu499 to His in the transmembrane domain of cynomolgus monkey c-Mpl results in the appearance of Mpl agonist activity for SKF-57626, which also possesses HuMpl agonistic activity and does not cause any reactions with cynomolgus monkey c-Mpl,[28] supporting the role of a His residue in the c-Mpl transmembraine domain. Onishi et al previously demonstrated that the point mutation of Ser505 to Asn in the HuMpl transmembrane domain creates a constitutively active form of the receptor,[29] and patients with familial essential thrombocythemia have recently been shown to possess this mutation.[30] Furthermore, mutating Val449 to Gln in the transmembrane domain constitutively activates Huβc.[31] We speculate that mutation in the transmembraine domain of the cytokine receptors may change their conformation and sensitivity to ligand binding or autophosphorylation. Although EPO receptor and growth hormone receptor have been reported to exist in a dimeric form prior to ligand binding,[32,33] no such evidence exists for c-Mpl. Because we have not yet confirmed whether NIP-004 binds directly to HuMpl, further investigation is needed to elucidate its exact mechanisms.

Analysis of human megakaryopoiesis and thrombopoiesis in vivo has been limited to xenotransplantation models, because continual, reproducible reconstruction of human platelet production is difficult using NOD/severe combined immunodeficiency (SCID) or NOD/SCID/β_2m^{null} mice. Perez et al demonstrated that human megakaryopoiesis and thrombopoiesis appeared 1 month after transplantation, and human platelets in these mice were functional using PB-derived $CD34^+$-transplanted NOD/SCID mice.[34] Human platelets were hardly detected in NOD/SCID mice receiving transplants of human CB cells.[34,35] Reconstitution of human megakaryopoiesis was also limited in NOD/SCID/β_2m^{null} mice.[36] We detected human platelets in all animals for 6 months after transplantation with CB-derived $CD34^+$ cells into NOG mice. We therefore believe that the NOG mouse is a suitable animal model for the analysis of human megakaryopoiesis and thrombopoiesis. TPO and c-Mpl are important molecules for megakaryopoiesis and thrombopoiesis. Administration of TPO can induce polyploid megakaryocytes in BM and increase the number of circulating platelets in mice and patients. In contrast, administration of TPO to NOD/SCID mice receiving xenotransplants with human hematopoietic progenitor cells does not alter the number of human platelets.[35] The present study demonstrated that NIP-004 increases the number of human platelets in NOG mice by significantly stimulating human megakaryopoiesis. To the best of our knowledge, this is the first report to demonstrate alteration of human megakaryopoiesis and thrombopoiesis in an animal model of xenotransplantation through c-Mpl activation. In our preliminary data, another TPO mimetic, SB-497115, which has been demonstrated to increase the number of platelets in healthy volunteers,[10] increased the number of circulating $HuCD41a^+$ platelets in NOG mice receiving xenotransplants (data not shown). In conclusion, we demonstrate that NIP-004 acts as a HuMpl activator to enhance CFU-MK formation in vitro and platelet production in vivo. Our new experimental animal model of human megakaryopoiesis may be a useful tool to study megakaryopoiesis in vivo.

Acknowledgments

We thank Dr Kenneth Kaushansky for his critical review, K. Miyaji for chemical construction of the compound, Y. Hirai for construction of HuGCSFR, and A. Ikejima for her technical assistance.

References

1 de Sauvage FJ, Hass PE, Spencer SD, et al. Stimulation of megakaryocytopoiesis and thrombopoiesis by the c-Mpl ligand. Nature. 1994;369:533-538.

2 Lok S, Kaushansky K, Holly RD, et al. Cloning and expression of murine thrombopoietin cDNA and stimulation of platelet production in vivo. Nature. 1994;369:565-568.

3 Kaushansky K, Lok S, Holly RD, et al. Promotion of megakaryocyte progenitor expansion and differentiation by the c-Mpl ligand thrombopoietin. Nature. 1994;369:568-571.

4 Wendling F, Maraskovsky E, Debili N, et al. cMpl ligand is a humoral regulator of megakaryocytopoiesis. Nature. 1994;369:571-574.

5 Bartley TD, Bogenberger J, Hunt P, et al. Identification and cloning of a megakaryocyte growth and development factor that is a ligand for the cytokine receptor Mpl. Cell. 1994;77:1117-1124.

6 Kaushansky K, Drachman JG. The molecular and cellular biology of thrombopoietin: the primary regulator of platelet production. Oncogene. 2002;21:3359-3367.

7 Kuter DJ, Begley CG. Recombinant human thrombopoietin: basic biology and evaluation of clinical studies. Blood. 2002;100:3457-3469.

8 Li J, Yang C, Xia Y, et al. Thrombocytopenia caused by the development of antibodies to thrombopoietin. Blood. 2001;98:3241-3248.

9 Ito M, Hiramatsu H, Kobayashi K, et al. NOD/SCID/gamma(c)(null) mouse: an excellent recipient mouse model for engraftment of human cells. Blood. 2002;100:3175-3182.

10 Jenkins J, Nicholl R, Williams D, et al. An oral, non-petide, small molecule thrombopoietin receptor agonist increases platelet counts in healthy subjects [abstract]. Blood. 2004;104:797a. Abstract 2916.

11 Jackson CW. Cholinesterase as a possible marker for early cells of the megakaryocytic series. Blood. 1973;42:413-421.

12 Matsumoto A, Masuhara M, Mitsui K, et al. CIS, a cytokine inducible SH2 protein, is a target of the JAK-STAT5 pathway and modulates STAT5 activation. Blood. 1997;89:3148-3154.

13 Suzuki H, Yamazaki H, Tanoue K. Immunocytochemical studies on co-localization of alpha granule membrane alphaIIbbeta3 integrin and intragranular fibrinogen of human platelets and their cell-surface expression during the thrombin induced release reaction. J Electron Microsc (Tokyo). 2003;52:183-195.

14 Hagberg IA, Lyberg T. Blood platelet activation evaluated by flow cytometry: optimised methods for clinical studies. Platelets. 2000;11:137-150.

15 Guideline for animal experimentation [in japanese]. Exp Anim. 1987;36:285-288.

16 Komatsu N, Kunitama M, Yamada M, et al. Establishment and characterization of the thrombopoietin dependent megakaryocytic cell line, UT-7/TPO. Blood. 1996;87:4552-4560.

17 Komatsu N, Nakauchi H, Miwa A, et al. Establishment and characterization of a human leukemic cell line with megakaryocytic features: dependency on granulocyte-macrophage colony stimulating factor, interleukin 3, or erythropoietin for growth and survival. Cancer Res. 1991;51:341-348.

18 Takatoku M, Kametaka M, Shimizu R, Miura Y, Komatsu N. Identification of functional domains of the human thrombopoietin receptor required for growth and differentiation of megakaryocytic cells. J Biol Chem. 1997;272:7259-7263.

19 Komatsu N, Yamamoto M, Fujita H, et al. Establishment and characterization of an erythropoietin-dependent subline, UT-7/Epo, derived from human leukemia cell line, UT-7. Blood. 1993;82:456-464.

20 Vainchenker W, Deschamps JF, Bastin JM, et al. Two monoclonal antiplatelet antibodies as markers of human megakaryocyte maturation: immunofluorescent staining and platelet peroxidase detection in megakaryocyte colonies and in in vivo cells from normal and leukemic patients. Blood. 1982;59:514-521.

21 van den Oudenrijn S, von dem Borne AE, de Haas M. Differences in megakaryocyte expansion potential between CD34( ) stem cells derived from cord blood, peripheral blood, and bone marrow from adults and children. Exp Hematol. 2000;28:1054-1061.

22 Kimura T, Kaburaki H, Tsujino T, Ikeda Y, Kato H, Watanabe Y. A non-peptide compound which can mimic the effect of thrombopoietin via c-Mpl. FEBS Lett. 1998;428:250-254.

23 Duffy KJ, Price AT, Delorme E, et al. Identification of a pharmacophore for thrombopoietic activity of small, non-peptidyl molecules: 2. Rational design of naphtho[1,2-d]imidazole thrombopoietin mimics. J Med Chem. 2002;45:3576-3578.

24 Duffy KJ, Darcy MG, Delorme E, et al. Hydrazinonaphthalene and azonaphthalene thrombopoietin mimics are nonpeptidyl promoters of megakaryocytopoiesis. J Med Chem. 2001;44:3730-3745.

25 Inagaki K, Oda T, Naka Y, Shinkai H, Komatsu N, Iwamura H. Induction of megakaryocytopoiesis and thrombocytopoiesis by JTZ-132, a novel small molecule with thrombopoietin mimetic activities. Blood. 2004;104:58-64.

26 Sakai R, Nakamura T, Nishino T, et al. Xanthocullins as thrombopoietin mimetic small molecules. Bioorg Med Chem. 2005;13:6388-6393.

27 Erickson-Miller CL, DeLorme E, Tian SS, et al. Discovery and characterization of a selective nonpeptidyl thrombopoietin receptor agonist. Exp Hematol. 2005;33:85-93.

28 Erickson-Miller CL, Delorme E, Iskander M, et al. Species specificity and receptor domain interaction of a small molecule TPO receptor agonist [abstract]. Blood. 2004;104:795a.

29 Onishi M, Mui AL, Morikawa Y, et al. Identification of an oncogenic form of the thrombopoietin receptor MPL using retrovirus-mediated gene transfer. Blood. 1996;88:1399-1406.

30 Ding J, Komatsu H, Wakita A, et al. Familial essential thrombocythemia associated with a dominant-positive activating mutation of the c-MPL gene, which encodes for the receptor for thrombopoietin. Blood. 2004;103:4198-4200.

31 Jenkins BJ, D'Andrea R, Gonda TJ. Activating point mutations in the common beta subunit of the human GM-CSF, IL-3 and IL-5 receptors suggest the involvement of beta subunit dimerization and cell type-specific molecules in signalling. EMBO J. 1995;14:4276-4287.

32 Constantinescu SN, Keren T, Socolovsky M, Nam H, Henis YI, Lodish HF. Ligand-independent oligomerization of cell-surface erythropoietin receptor is mediated by the transmembrane domain. Proc Natl Acad Sci U S A. 2001;98:4379-4384.

33 Brown RJ, Adams JJ, Pelekanos RA, et al. Model for growth hormone receptor activation based on subunit rotation within a receptor dimer. Nat Struct Mol Biol. 2005;12:814-821.

34 Perez LE, Rinder HM, Wang C, Tracey JB, Maun N, Krause DS. Xenotransplantation of immunodeficient mice with mobilized human blood CD34 cells provides an in vivo model for human megakaryocytopoiesis and platelet production. Blood. 2001;97:1635-1643.

35 Perez LE, Alpdogan O, Shieh JH, et al. Increased plasma levels of stromal-derived factor 1 (SDF-1/CXCL12) enhance human thrombopoiesis and mobilize human colony-forming cells (CFC) in NOD/SCID mice. Exp Hematol. 2004;32:300-307.

36 Angelopoulou MK, Rinder H, Wang C, Burtness B, Cooper DL, Krause DS. A preclinical xenotransplantation animal model to assess human hematopoietic stem cell engraftment. Transfusion. 2004;44:555-566.

ELSEVIER

EXPERIMENTAL HEMATOLOGY

Experimental Hematology 34 (2006) 1239–1247

Development of human–human hybridoma from anti-Her-2 peptide–producing B cells in immunized NOG mouse

Yoshie Kametani[a,f], Masashi Shiina[a], Ikumi Katano[a], Ryoji Ito[a], Kiyoshi Ando[b], Kanae Toyama[a], Hideo Tsukamoto[c], Takuya Matsumura[a], Yuki Saito[d], Dai Ishikawa[g], Takao Taki[g], Mamoru Ito[h], Kohzoh Imai[i], Yutaka Tokuda[d], Shunichi Kato[e], Norikazu Tamaoki[h], and Sonoko Habu[a,f]

[a]*Department of Immunology;* [b]*Department of Hematology and Oncology;* [c]*Laboratory for Molecular Science Research;* [d]*Department of Surgery;* [e]*Department of Pediatrics;* [f]*Center for Embryogenesis and Organogenesis, Tokai University School of Medicine, Kanagawa, Japan;* [g]*Molecular Medical Science Institute, Otsuka Pharmaceutical Co. Ltd., Tokushima, Japan;* [h]*Central Institute for Experimental Animals, Kanagawa, Japan;* [i]*First Department of Internal Medicine, Sapporo Medical University, Hokkaido, Japan*

(Received 3 December 2005; revised 24 April 2006; accepted 4 May 2006)

Objective. **Numerous monoclonal antibodies have been developed for the purpose of medical treatments, including cancer treatment. For clinical application, the most useful are human-derived antibodies. In this study, we tried to prepare designed antigen-specific antibodies of completely human origin using immunodeficient mouse.**

Methods. **Nonobese diabetic/severe combined immunodeficient/IL-2 receptor γ null mouse (NOG) mouse was used to reconstitute the human immune system with umbilical cord blood hematopoietic stem cells (CB-NOG mouse) and to prepare human-derived Her-2-epitope–specific antibodies. Hybridoma lines were prepared by fusing the human myeloma cell line Karpas707H.**

Results. **Serum of immunized NOG mouse contained human-derived immunoglobulin M (IgM) antibodies specific for a short peptide sequence of 20 amino acids, including the epitope peptide of apoptotic Her-2 antibody CH401. Hybridoma lines were successfully prepared with spleen B cells obtained from the immunized CB-NOG mouse. One of these cell lines produced human IgM against the epitope peptide that can recognize surface Her-2 molecule.**

Conclusion. **We could produce human-derived IgM antibody against Her-2 epitope peptide in CB-NOG mouse, succeeding in generation of human hybridoma-secreting IgM against a given peptide.**

Passive monoclonal antibody (mAb) therapy has been accepted as a treatment for cancers and autoimmune diseases for the past decade [1,2]. For patients affected by cancer, passive mAb therapy is of benefit mainly because the immune reaction of most patients is suppressive. To date, several antibodies such as Trastuzumab (Herceptin) and Rituximab have been already under practical use, and some are under clinical investigation. Therapeutic effectiveness of these antibodies, to some extent, promotes development of new monoclonal antibodies related to the disease [3]. In addition to cancer patients, anti-tumor necrosis factor-α mAb of human–mouse chimera mAb (Infliximab), or of completely humanized mAb (Adalimumab) are used for suppression of T-cell function in rheumatoid arthritis and Crohn's disease, and are proved to be relatively successful [4,5].

In consideration of clinical application, therapeutic antibody is ideal to be humanized. Today, almost all antibodies for clinical use are derived from mouse, at least in part, although they were humanized by techniques of molecular biology [6]. Recently, the mouse line carrying human chromosome fragments containing immunoglobulin (Ig) gene cluster was developed, which made it possible to prepare completely human-type antibodies produced by mouse B cells [7]. However, these mice produce IgG with sugar chains of mouse origin. Although sugar chains are

Offprint requests to: Sonoko Habu, M.D., Ph.D., Department of Immunology, Tokai University School of Medicine, Boseidai, Isehara, Kanagawa, 259-1193 Japan; E-mail: sonoko@is.icc.u-tokai.ac.jp

0301-472X/06 $–see front matter.
doi: 10.1016/j.exphem.2006.05.006

thought to have low immunoreactivity induced by species-specificity, the risk to induce human anti-mouse antibody production remains [8]. Therefore, the most ideal system is that of antibodies of human origin produced by human B cells.

We have developed a human immune system reconstituted in the mouse environment by transplanting human hematopoietic stem cells in immunodeficient mouse [9,10]. In comparison with nonobese diabetic-severe combined immunodeficient (NOD-SCID) mice, NOD-SCID–IL-2Rγ knockout mouse (NOG) showed higher engraftment of human hematopoietic cells and higher proportion of T-cell development in the xenogenetic environment [11]. In a previous study, we reconstituted the human immune system in NOG mouse with umbilical cord blood hematopoietic stem cells (CB-NOG) and found that immunization of 2,4-dinitrophenol-conjugated keyhole limpet hemocyanin (DNP-KLH) induces antigen-specific human IgM production [12]. These findings indicate that the reconstituted human immune system has developed potential for producing antibodies against the immunized antigens, although the net number of human T and B cells per head in CB-NOG mice is less than one tenth that in normal mouse.

To obtain human-derived antibody to effectively suppress tumor cells or mass, we can immunize CB-NOG mice with a particular epitope, which is recognized by an apoptotic antibody. Among the reported monoclonal antibodies against Her-2 established by mouse and the epitopes reported [13–16], some possessed suppressive effect for tumor growth. Ishida and collaborators [17] established a humanized monoclonal antibody termed CH401, which has an epitope different from Herceptin and induces apoptosis to Her-2–expressing cells efficiently. In this article, we focus on the capacity of human B cells developed in mouse environment to produce antigen-specific antibodies, to analyze if CH401-recognizing epitope can induce human B cells to produce epitope-specific antibody in CB-NOG mouse. As a result, we determined that the CB-NOG mouse produced specific antibodies against a short peptide of 20 amino acids carrying the CH401 epitope. Consequently, the antibody-producing B cells were fused with a human myeloma cell line, Karpas707H [18], to establish a hybridoma line.

Materials and methods

Mice

NOD/Shi-scid, common γc-null (NOD/SCID/γc-null; NOG) mice were provided from the Central Institute for Experimental Animals (Kawasaki, Japan). BALB/c mice were purchased from Crea Japan Inc. (Kawasaki, Japan). All mice were kept under specific pathogen-free conditions in the animal faculty located at the Tokai University School of Medicine (Isehara, Japan).

Human hematopoietic stem cells

Human umbilical cord blood was obtained from full-term healthy newborns immediately after vaginal delivery. Informed consents were obtained according to Institute guidelines, and this work was approved by Tokai University Human Research Committee. Mononuclear cells (MNCs) were separated by Ficoll-Paque gradient centrifugation. $CD34^+$ cells were purified from MNCs using the two-step MACS system (Miltenyi Biotec, Gladbach, Germany). The purity was >98%.

Transplantation

Nine-week-old NOG mice were irradiated sublethally with 2.5 Gy prior to transplantation, and $CD34^+$ cells were transplanted intravenously. Eight weeks after transplantation, peripheral blood was collected via orbit under inhalation anesthesia. MNCs were prepared and reconstitution efficiencies were calculated by hCD45 expression analyzed by fluorescein-activated cell sorting (FACS) analysis.

Peptides

Her-2 peptide includes the sequence identified as the epitope of an apoptotic anti-Her-2 antibody, CH401, which was determined using multiple antigen peptides (MAP) peptides with a partial amino acid sequence of Her-2 (Miyako et al., manuscript in preparation). The sequence of the peptide is N:163-182 ((YQDTILWK-DIFHKNNQLALT-BBB)8-K4K2KB). This peptide was synthesized using Rink amide resin (0.4–0.7 mmol/g) and peptide synthesizer ACT357 (Advanced Chemtech, Louisville, KY, USA). On the 96-well plate, each of these MAP peptides was coated and the cross-reactivity with CH401 was examined by enzyme-linked immunosorbent assay (ELISA).

Monoclonal antibodies, flow cytometry, and cell sorting

All cells were analyzed using FACS Calibur (Becton Dickinson, Franklin Lakes, NJ, USA). For each analysis or sorting, living gate white blood cells or lymphocytes were further gated on human $CD45^+$ cells. Mouse anti-human mAbs included peridinine chlorophyll protein-conjugated CD45, T-cell receptor (TCR), CD1a, fluorescein isothiocyanate (FITC)-conjugated CD4, IgM, phycoerythrin-conjugated CD4, CD8, IgD, and allophycocyanin (APC)-conjugated CD19.

Immunization, EBV transformation, and hybridoma preparation

Eight to 10 weeks after transplantation, mice were immunized intraperitoneally with 2,4-dinitrophenylated keyhole limpet haemocyanin (DNP-KLH; 100 μg/alum/head), toxic shock syndrome toxin-1 (TSST-1; 25 μg/alum/head), Her-2 extracellular domain (25 μg/alum/head) or Her-2 epitope peptide (100 μg/FCA/head). Mice were immunized every 2 weeks. Four days after the last booster, mice were sacrificed and spleen cells were collected. Epstein-Barr virus (EBV) transformation was performed by conventional method. Four weeks after EBV treatment, culture supernatants were collected and specific-antibody–producing clones were selected by ELISA, as described previously [9]. The cells secreting specific antibodies were expanded and fused with a human myeloma cell line, Karpas707H, using polyethylene glycol. Hybridomas were selected by Ouabine and HAT. Positive clones were selected by ELISA.

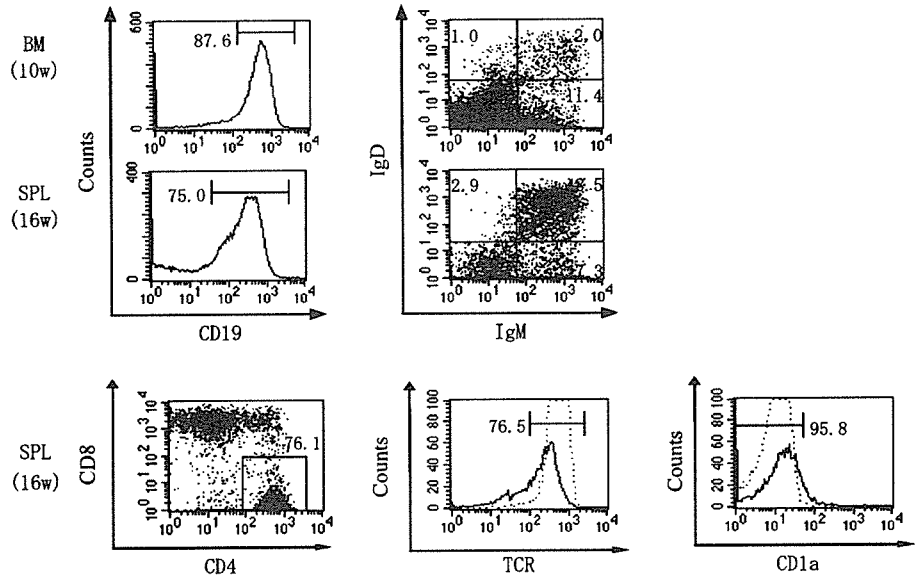

Figure 1. Reconstitution of human immune system in nonobese diabetic/severe combined immunodeficient/gammac(null) mouse with umbilical cord blood $CD34^+$ cells. Fluorescein-activated cell sorting analysis of lymphoid tissue cells. Bone marrow (BM) cells were prepared 10 weeks after transplantation. Spleen (SPL) cells were prepared 16 weeks after transplantation. CD4SP cells were enclosed in a square and the percentage was shown above the square. T-cell receptor (TCR) and CD1a expression was analyzed for the CD4SP-gated fractions. B cells were gated for $CD19^+$ cells, and immunoglobulin (Ig) IgM and IgD double-staining patterns are shown.

Results

CB-NOG can produce specific antibodies against ordinary protein antigens

We reported previously that IgM+IgD+mature type human B cells are detectable in the spleen and bone marrow of NOG mouse reconstituted with CB-derived $CD34^+$ cells (CB-NOG mouse), although the majority of IgM^+ cells in bone marrow are IgD-negative immature B cells [12]. In addition, as shown in Figure 1 of this study, the spleen of these CB-NOG mice were shown to contain CD4 and CD8 single-positive human T cells, with high expression of TCR. The pattern of mature T and B cells as shown in Figure 1 was observed in the mice with relatively high reconstitution ratio of human-derived cells (>20%, data not shown). Thus, for examination of human antibody production specific to a given antigen, we used CB-NOG mice, the engraftment of which was >20% in the 8th to 10th week after transplantation of human CB cells. These CB-NOG mice were immunized with Her-2 extracellular domain (exHer-2), DNP-KLH as a hapten-carrier system, or whole protein TSST-1 intraperitoneally with alum biweekly (Fig. 2A). Two experiments were performed using CB-NOG mouse groups, each of which was transplanted with one-donor–derived $CD34^+$ cells (Table 1).

Antigen-specific IgM was detected in the sera of mice immunized with three kinds of antigens in both experiments, but specific IgG was not detected even after five boosters in all CB-NOG mice (data not shown). Reconstitution efficiency, which was determined by the proportion of human $CD45^+$ cells in the peripheral blood and specific IgM producibility were not statistically correlated in the immunized mice (Fig. 2B). Moreover, the immunized CB-NOG mouse showed very little positive correlation between total serum IgM and specific IgM producibility (Fig. 2C). Among the immunized mice with each protein antigen, the ratio of mice producing specific antibody against exHer-2 was lower (3/6) in comparison with that of mice immunized with DNP-KLH (4/4) and TSST-1 (2/2 in experiment 1 and 7/11 in experiment 2) (Table 1).

Detection of human IgM antibody specific for Her-2-peptide antigen

We have previously reported on the preparation of a humanized antibody termed CH401, which recognizes extracellular domain of Her-2 different from the recognition site of Herceptin [19]. Moreover, we recently identified an epitope peptide recognized by CH401 (Miyako et al., manuscript in preparation). In consideration of the clinical application of oligo-clonal antibodies carrying various epitopes, such epitope-specific antibodies would be useful. Then, we tried to raise the specific IgM antibody against an epitope peptide of CH401 in the immunized CB-NOG mice based on the above result that CB-NOG mice can produce human-derived IgM antibodies specific for the immunized exHer-2 protein antigen. However, because Her-2 is originally a membrane protein, the question remained whether immunization of a Her-2–derived peptide could promote production of antibodies against the CH401 epitope peptide (20 amino residues), which recognize Her-2 whole chain expressed on the cell surface. For that, we examined whether immunization of the peptide alone can induce efficiently specific antibody

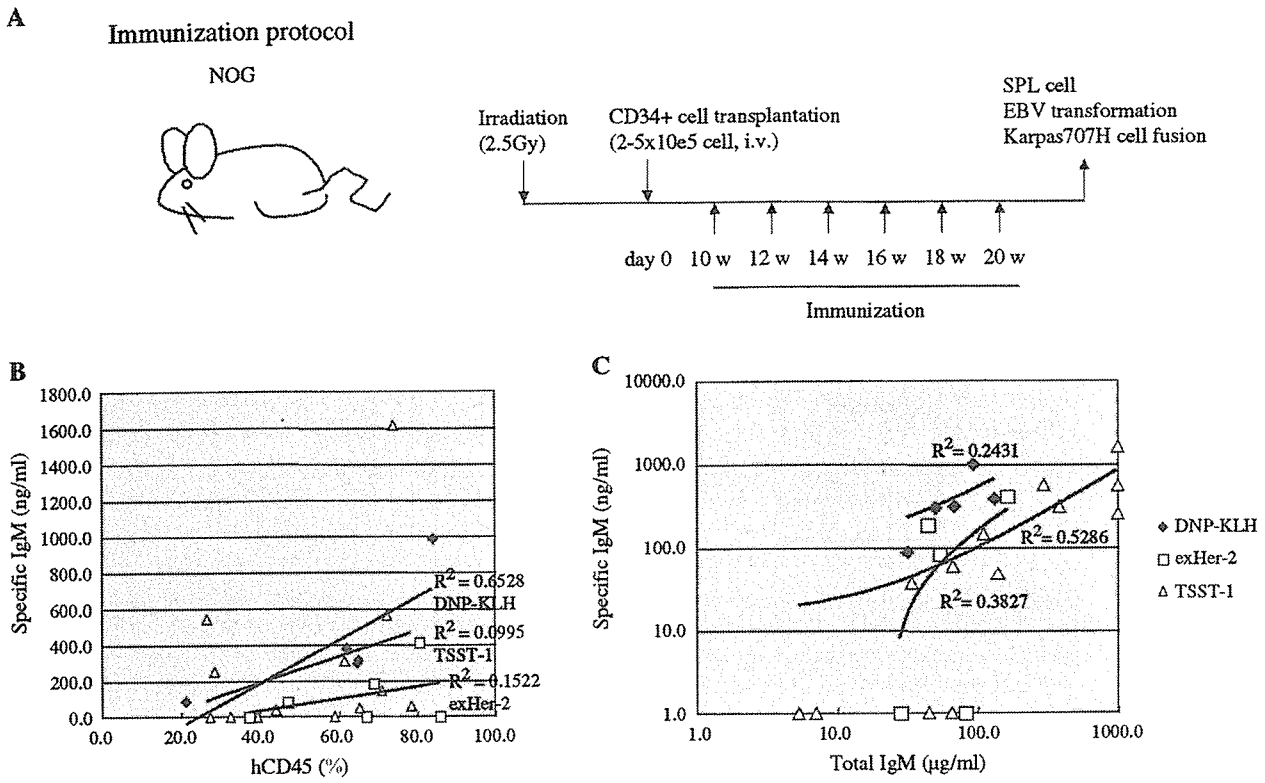

Figure 2. Correlation of specific antibody with reconstitution efficiency. (**A**) Nine-week-old nonobese diabetic/severe combined immunodeficient/gammac(null) (NOG) mice were irradiated and transplanted with $CD34^+$ cells purified from cord blood. Ten weeks after the transplantation, immunization was started biweekly. Four days after the last booster, splenocytes were prepared and fused with Karpas707H. (**B**) Specific immunoglobulin M (IgM) of the mice vs hCD45 (%) of the mice for experiment 1 data. $R^2 = 0.6528$ for 2,4-dinitrophenol-conjugated keyhole-limpet-hemocyanin (DNP-KLH), $R^2 = 0.1522$ for exHer-2, $R^2 = 0.0995$ for toxic shock syndrome toxin-1 (TSST-1). Totally not so high correlation between the concentration of specific antibodies and efficiency of engraftment was observed. (**C**) Specific IgM/total IgM were analyzed for experiment 1 data shown in Table 1. Samples with specific antibodies were used for estimating the coefficients of correlation. $R^2 = 0.2431$ for DNP-KLH, $R^2 = 0.3827$ for Her-2, $R^2 = 0.5286$ for TSST-1.

production or whether co-immunization with cells expressing Her-2 on their surface provides synergistic or additional effect on anti-peptide antibody production. An immunization protocol we performed was shown in Figure 2A and Table 2. For peptide immunization, we used MAP because MAP peptides were reported to have similar immunogenicities to hapten-carrier antigens [20,21].

Ten and 20 weeks after $CD34^+$ cell transplantation (pre-immunization and a week after the fifth immunization), sera were collected and ELISA was performed for measuring serum level of anti-peptide antibodies (Table 3). In experiment 2-1, 16 NOG mice transplanted with human CB cells obtained from one donor were divided into three groups and immunized with epitope peptide alone (P), SV22, a NIH3T3-derived cell line expressing Her-2 (S), or epitope peptide plus SV22 (P/S), respectively. Peptide-specific IgM antibody was substantially detectable in 2/3 CB-NOG mice receiving epitope peptide alone. In comparison, immunization of SV22 or of SV22 plus epitope peptide led the ratio of anti-peptide–producing mice to 100%. The similar tendency was found in experiment 2-2, in which CB-NOG mice received another donor-derived $CD34^+$ CB cells. These results showed that a peptide immunization is capable of producing the peptide-specific antibody in CB-NOG mice. Although the ratio of antibody-producing mice was higher in mice immunized with SV22 cells plus peptide than in mice immunized with peptide alone, the same high efficiency was also found with immunization with SV22 cells, suggesting that the Her-2 epitope has sufficient antigenicity in the whole Her-2 molecule on the cell surface without additional immunization with the peptide.

Human hybridoma preparation using human myeloma cell line Karpas707H

Next, we tried to establish human–human hybridoma by fusing B cells prepared from the spleen of immunized CB-NOG mouse with a human myeloma cell line. As for human myeloma cell line, Karpas707H was used. Specificity of antibodies secreted in the culture supernatant was analyzed by ELISA, results of which are shown in Table 4. Only four Her-2–specific hybridoma lines were obtained from the mice immunized with exHer-2, while 32 hybridoma lines were obtained for DNP-KLH specific B cells. As CB-NOG mice produce mainly IgM isotype for antigen-specific antibody, spleen cells of the mice immunized with Her-2 peptide and SV22 were transformed with EBV before the fusion with

Table 1. Summary of specific antibody production in CB-NOG

Ag	Total IgM (μg/mL)	hCD45 (%)	Specific IgM (ng/mL)
	Experiment 1-1		
DNP-KLH	131.9	62.0	375.3
DNP-KLH	93.4	84.1	981.8
DNP-KLH	50.2	64.8	294.7
DNP-KLH	31.9	21.4	86.0
exHer-2	162.8	80.7	409.5
exHer-2	110.7	37.4	0.0
exHer-2	54.1	47.0	81.8
exHer-2	44.7	69.0	182.5
exHer-2	28.5	67.1	0.0
exHer-2	82.2	86.0	0.0
TSST-1	139.2	65.3	47.9
TSST-1	34.2	44.1	36.8
	Experiment 1-2		
TSST-1	>1000	26.6	543.1
TSST-1	>1000	28.5	250.3
TSST-1	>1000	74.1	1610.4
TSST-1	110.1	71.1	143.4
TSST-1	295.8	72.4	561.0
TSST-1	381.3	61.5	305.3
TSST-1	65.9	59.0	0.0
TSST-1	45.2	32.7	0.0
TSST-1	67.1	78.7	58.5
TSST-1	5.3	27.4	0.0
TSST-1	7.0	39.5	0.0

Total immunoglobulin M (IgM), specific IgM, and percentage of human $CD45^+$ cells in bone marrow were compared. Percentage of $CD45^+$ cells was determined by fluorescein-activated cell sorting. Total and specific IgM levels were determined by enzyme-linked immunosorbent assay.
CB-NOG = NOG mouse reconstituted with CB-derived $CD34^+$ cells; DNP-KLH = 2,4-dinitrophenol-conjugated keyhole-limpet-hemocyanin; exHer-2 = Her-2 extracellular domain; TSST-1= toxic shock syndrome toxin-1.

Karpas707H. As a result, we obtained specific antibody-producing hybridoma lines in both experiments, with or without EBV treatment. Consequently, totally 20 hybridoma lines producing peptide-specific antibody were obtained from the mice of experiment 2-1 (P/S-1, S and P/S-2). Moreover, 28 peptide-specific IgM-producing hybridoma lines were obtained in P/S-3 mice (experiment 2-2). One of these clones was expanded and anti-peptide IgM was collected from the supernatants. FACS analysis showed that the antibody specifically recognized surface Her-2 expressed on A20, though the intensity was not so high as that of Herceptin (Fig. 3). However, we could not detect any apoptotic effect of this antibody on Her-2–expressing cancer cells under the presence of human complement (data not shown).

These results suggest that NOG mice can produce antigen-specific IgM against very short epitope peptides. Antibody-producing B cells were successfully fused with a human myeloma cell line, and antibody-producing hybridoma was obtained. Using this system, we prepared hybridoma lines of completely human type secreting anti-Her-2 IgM.

Discussion

There is increasing evidence showing that clinical trials of certain humanized monoclonal antibodies are prospective [1,2], although their therapeutic effect is not always constitutive [22]. On the other hand, there is an argument that such antibodies may cause production of new anti-mouse antibodies during the continuous treatments because most of the therapeutic antibodies are generated from the human-mouse chimera antibody [8]. In this study, we examined the capacity of human B cells developed in mouse environment to produce antigen-specific antibodies, particularly against certain peptides, in vivo. For this, the human immune

Table 2. Immunization protocol for Her-2–related antigens

Group	Immunization no. 1	2	3	4	5
	Experiment 2-1				
1 (P)	Peptide	Peptide	Peptide	Peptide	Peptide
2 (P/S)	Peptide	Peptide	Peptide	SV22	SV22
3 (S)				SV22	SV22
	Experiment 2-2				
1 (P)	Peptide	Peptide	Peptide	Peptide	Peptide
2 (P/S)	Peptide	Peptide	Peptide	SV22	SV22
3 (H)	Her-2	Her-2	Her-2	Her-2	Her-2
4 (H/S)	Her-2	Her-2	Her-2	SV22	SV22
5 (S)				SV22	SV22

CB-NOG mice were immunized with Her-2–related antigens. In the experiment 2-1, epitope peptide and SV22 were used for the priming and booster. In the experiment 2-2, recombinant Her-2 extracellular domain protein (exHer-2) was also used.
CB-NOG = NOG mouse reconstituted with CB-derived $CD34^+$ cells; H = exHer-2; H/S = exHer-2 and SV22; P = peptide; P/S = peptide and SV22; S = SV22.

Table 3. Summary of anti-Her-2 antibody production in CB-NOG mice

	Experiment 2-1					
	10 Weeks after transplantation		20 Week after transplantation			
Ag	Total IgM (μg/mL)	hCD45 (%)	Total IgM (μg/mL)	Total IgG (ng/mL)	Her-2 IgM (ng/mL)	Anti-Peptide IgM (ng/mL)
P	90.7	81.4	287.9	13,548.9	0	334.4
P	58.2	30.8	418.6	2533.3	0	0
P	76.6	62.6	308.9	22,379.7	0	34.2
P/S	28	85.0	98.8	1237	18	138.4
P/S	153.7	82.1	373.4	55	0	65
P/S	104.9	88.3	185.6	26,855.3	0	59.2
P/S	94.1	83.7	250.2	0.361	0	53.6
P/S	98.2	63.8	228.2	10,788.9	0	60.7
P/S	123	63.0	208.4	0	0	52
P/S	7.6	51.8	96	0	3.6	50.4
P/S	55.7	45.5	368.3	0	0	37.6
P/S	325.1	64.5	424.8	0	0	111.2
P/S	133.6	71.1	166.9	0	0	106.9
S	47.5	72.8	194.8	801.2	0	153.7
S	108.6	61.8	324.1	4866.8	0	48.7
S	108.6	29.8	231	411.3	0	143.6
	Experiment 2-2					
P		88.3			0.0	0.0
P		80.5			0.0	0.0
P/S		83.0			0.0	5.0
P/S		57.1			0.0	12.5
P/S		90.1			0.0	0.0
P/S		39.5			725.9	613.8
H	ND	64.9	ND	ND	0.0	129.8
H		52.1			0.0	0.0
H		93.8			0.0	0.0
H		74.1			0.0	29.0
H/S		70.4			0.0	0.0
H/S		94.7			0.0	193.3
S		87.4			0.0	234.5
S		77.4			0.0	30.6

CB-NOG mice were immunized by the protocols as shown in Table 2. Total immunoglobulin M (IgM) and hCD45 (%) were determined 10 weeks after transplantation. Specific IgM, total IgM, and total IgG were determined at week 20.
CB-NOG = NOG mouse reconstituted with CB-derived $CD34^+$ cells; H = exHer-2; Her-2 = exHer-2 used for enzyme-linked immunosorbent assay (ELISA); H/S = exHer-2 and SV22; ND = not determined; P = peptide; Peptide = epitope peptide used for ELISA; P/S = peptide and SV22; S = SV22.

system in immunodeficient mouse was reconstituted by transplantation of human cord blood $CD34^+$ cells (CB-NOG), and they were thereafter immunized with given antigens. Then, antibody-producing human B cells obtained from the spleen of immunized CB-NOG mice were fused with a human myeloma cell line, which was recently established by Karpas et al. [18] to generate human–human hybridoma.

Among immunodeficient mice used for transplantation of human tissues, NOG mice were reported to be the most acceptable for human leukocytes [11]. Moreover, several groups including us showed that the human immune system could be efficiently reconstituted in NOG mice after transplantation of $CD34^+$ human cord blood cells [10,12,23,24]. Moreover, we demonstrated that the CB-NOG mice produced the antigen-specific antibody when they were immunized with DNP-KLH [12]. In this study, we examined whether peptide-specific antibodies are produced in the reconstituted CB-NOG mice when they were immunized with a MAP peptide with a small region of the Her-2 epitope peptide in Freund's complete adjuvant. In these mice, IgM production against a given short peptide antigen was detected with a relatively high frequency, which was not different from that of mice immunized with the ordinary protein antigens, such as a Her-2 extracellular domain. Compared with the peptide immunization, tumor cells expressing Her-2 on their surface induced anti-Her-2 peptide antibody production in a markedly high frequency. Peptide immunization did not have additive effect on the specific antibody induction when the Her-2–expressing cells were used for the antigen, as the frequency of antibody-producing mice and the antibody concentration in the sera were

Table 4. Summary of hybridoma production by CB-NOG B cells and Karpas707H

Ag	Mouse[a]	EBV	Cell[b] (x10e5)	Colony (n)	Total antibody (colony, n)		Specific antibody (colony, n)	
					IgM	IgG	IgM	IgG
H	4	-	921	142	21	15	4	ND
P/S-1	1	+	366	31	ND	ND	8	ND
P/S-2	1	+	255	14	ND	ND	2	ND
P/S-3	1	+	641	54	ND	ND	28	ND
S	1	+	358	48	ND	ND	10	ND
DNP-KLH	4	-	351	58	32	0	32	0

CB-NOG B cells were fused with Karpas707H and the yield was shown.
CB-NOG = NOG mouse reconstituted with CB-derived $CD34^+$ cells; DNP-KLH = 2,4-dinitrophenol-conjugated keyhole-limpet-hemocyanin; EBV = Epstein-Barr virus; H = exHer-2; Ig = immunoglobulin; ND = not determined; P/S = peptide and SV22; S = SV22.
Antibody production was determined by enzyme-linked immunosorbent assay for culture supernatants. Four clones were exHer-2–specific. Forty-eight clones were epitope peptide-specific. One of the clones stably produced antibodies for more than 7 months.
[a]Mouse pooled for one fusion experiment.
[b]Total cell number used for one fusion experiment.

not so different between the peptide-immunized and nonimmunized groups. These results indicate that immunization of a certain peptide derived from the membrane protein can induce specific antibodies in CB-NOG mice, but that its antigenicity is not as strong as the whole molecule including the epitope sequence expressed on the cell surface.

Only IgM was detectable as antigen-specific antibodies in the sera of CB-NOG mice when mice were immunized with either peptide or ordinary protein antigens. In consideration of the characters of CB-NOG mice, this result might not be unexpected: the majority of spleen B cells of CB-NOG are $CD5^+B1$ cells [12], which are recognized as being the major IgM producer. However, human B cells developed in CB-NOG mice have a potential to produce IgG, because nonspecific IgG was detected in the CB-NOG mice immunized with Her-2 peptide. Very recently, Ishiawa et al. [25] reported development of specific IgG against ovalbumin in newborn NOG mice receiving transplantation of human stem cells, although the antibody level was not high enough. Therefore, it is possible that the cognate interaction mediated by a certain antigen on major histocompatibility class (MHC) II between B cells and T cells may occur in a low frequency, presumably because most human T cells developed in the mouse thymus of CB-NOG mice are restricted with mouse MHC. Consequently, only a low proportion of B cells can recognize helper T cells by human MHC restriction to secrete antigen-specific IgG (in preparation).

To date, most human monoclonal antibodies were prepared from mouse–human hybridoma lines prepared by human B cells and mouse myeloma cell lines, mainly because the adequate human myeloma cell line was not available. Recently, Karpas and his collaborators established a myeloma cell line, Karpas707H, which expresses a low level of human light chain without its secretion. Using this myeloma cell line, they succeeded in establishing genuine

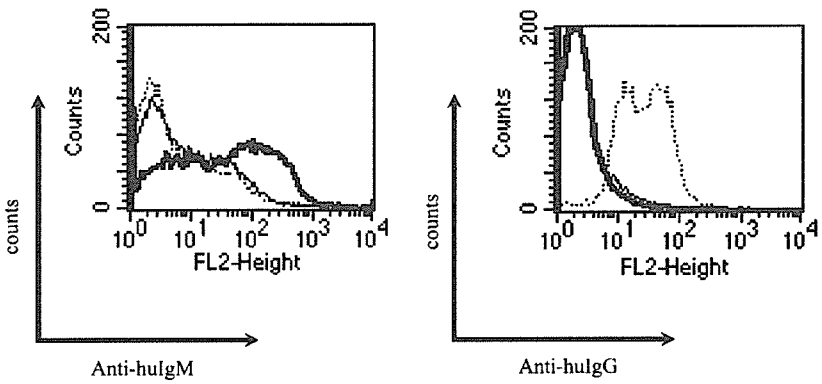

Figure 3. Recognition of surface Her-2 by human anti-Her-2 immunoglobulin M (IgM). Anti-Her-2 IgM was prepared from human hybridoma and purified. Mouse B-cell lymphoma (A20) expressing Her-2 was stained with the anti-peptide IgM antibody prepared from one of the hybridoma lines or Herceptin (IgG). Phycoerythrin-conjugated anti-human IgM (Anti-huIgM) or anti-human IgG (Anti-huIgG) was used for the secondary antibody. Cells were washed and analyzed by fluorescein-activated cell sorting analysis. Bold lines show the staining pattern with anti-peptide IgM; dotted lines show that of Herceptin. Solid thin lines show that of only secondary antibody.

human hybridomas by fusing with EBV transformed human B cell line producing anti-HIV-1 IgG and with fresh cells obtained from tonsils or peripheral blood cells. According to their process, we fused Karpas707H with spleen cells obtained from CB-NOG mice immunized with given antigens. Corresponding to the spectrum of the immunoglobulin type in the serum of the immunized CB-NOG mice, all the hybridomas we established secreted IgM antibody against Her-2 peptide (Table 4). Among these, one of the hybridoma lines maintained production of anti-Her-2 peptide antibody in the culture for more than 7 months without losing IgM secretion ability, and the partially purified antibody recognized Her-2 transfectants. Corresponding to the serum Igs, some of the hybridoma lines were found to secrete nonspecific IgG antibodies, indicating that at least EBV transformation of B cells in vitro does not disturb the fusion of Karpas707H with spleen B cells producing either IgG or IgM in CB-NOG.

IgG-type monoclonal antibody is considered more useful for clinical usage mainly because of its low molecular weight, high specificity, and multifunctions. However, IgM may not always be invalid for clinical application. For example, IgM antibodies against HIV induce more efficient cytolysis for infected cells in a complement-mediated manner presumably because the complement binding ability of IgM is higher than IgG [26]. Although our monoclonal IgM antibody showed very low cytotoxic activity against Her-2–positive tumor in vitro under the presence of mouse serum (data not shown), several groups reported that IgM antibodies possess anti-tumor function in the presence of complements [27–31]. Thus, the method described in this article will be useful in obtaining genuine human monoclonal antibody to the surface molecule on tumor cells, even if the antibody is IgM.

In summary, we demonstrated that CB-NOG mice, which were prepared from immunodeficient NOG mice reconstituted with human immune system, have potential for producing peptide-antigen–specific IgM antibodies, although most B cells developed in the mice are $CD5^+$ cells. We could produce human-derived IgM antibody against Her-2 epitope peptide in the CB-NOG mice. By fusing splenic B cells from the immunized NOG mice with a human myeloma cell line, we succeeded to generate genuine human hybridoma secreting antigen-specific IgM against a given peptide.

References

1. Osbourn J, Jermutus L, Duncan A. Current methods for the generation of human antibodies for the treatment of autoimmune diseases. Drug Discov Today. 2003;8:845–851.
2. Stern M, Herrmann R. Overview of monoclonal antibodies in cancer therapy: present and promise. Crit Rev Oncol/Hematol. 2005;54:11–29.
3. Glennie M, van de Winkel J. Renaissance of cancer therapeutic antibodies. Drug Discov Today. 2003;8:503–510.
4. Hochberg M, Lebwohl M, Plevy S, Hobbs K, Yocum D. The benefit/-risk profile of TNF-blocking agents: findings of a consensus panel. Semin Arthritis Rheum. 2005;34:819–836.
5. Botsios C. Safety of tumour necrosis factor and interleukin-1 blocking agents in rheumatic diseases. Autoimmun Rev. 2005;4:162–170.
6. Qu Z, Griffiths G, Wegener W, et al. Development of humanized antibodies as cancer therapeutics. Methods. 2005;36:84–95.
7. Tomizuka K, Shinohara T, Yoshieda H, et al. Double trans-chromosomic mice: maintenance of two individual human chromosome fragments containing Ig heavy and k loci and expression of fully human antibodies. Proc Natl Acad Sci U S A. 2000;97:722–727.
8. Mirick G, Bradt B, Denardo S, Denardo G. A review of human anti-globulin antibody (HAGA, HAMA, HACA, HAHA) responses to monoclonal anitbodies. Not four letter words. Q J Nucl Med Mol Imaging. 2004;48:251–257.
9. Li C, Ando K, Kametani Y, et al. Reconstitution of functional human B lymphocytes in NOD/SCID mice engrafted with ex vivo expanded CD34(+) cord blood cells. Exp Hematol. 2002;30:1036–1043.
10. Saito Y, Kametani Y, Hozumi K, et al. The in vivo development of human T cells from CD34(+) cells in the murine thymic environment. Int Immunol. 2002;14:1113–1124.
11. Ito M, Hiramatsu H, Kobayashi K, et al. NOD/SCID/gamma(c)(null) mouse: an excellent recipient mouse model for engagement of human cells. Blood. 2002;100:3175–3182.
12. Matumura T, Kametani Y, Ando K, et al. Functional CD5+ B cells develop predominantly in the spleen of NOD/SCID/gc^{null} (NOG) mice transplanted either with human umbilical cord blood, bone marrow, or mobilized peripheral blood CD34+ cells. Exp Hematol. 2003;31:789–797.
13. Lucchese A, Stevanovic S, Sinha A, Mitterlman A, Kanduc D. role of MHC II affinity and molecular mimicry in defining anti-HER-2/neu MAb-3 linear peptide epitope. Peptides. 2003;24:193–197.
14. Klapper L, Vaisman N, Hurwitz E, et al. A subclass of tumor-inhibitory monoclonal antibodies to ErbB-2/HER2 blocks crosstalk with growth factor receptors. Oncogene. 1997;14:2099–2109.
15. Shawver L, Mann E, Elliger S, Dugger E, Arteaga C. Ligand-like effects induced by anti-c-erbB-2 antibodies do not correlate with and are not required for growth inhibition of human carcinoma cells. Cancer Res. 1994;54:1367–1373.
16. Yip Y, Smith G, Koch J, Dubel S, Ward RL. Identification of epitope regions recognized by tumor inhibitory and stimulatory anti-ErbB-2 monoclonal anitbodies: implications for vaccine design. J Immunol. 2001;166:5271–5278.
17. Ishida T, Tsujisaki M, Hinoda Y, Imai K, Yachi A. Establishment and characterization of mouse-human chimeric monoclonal anitbody to *erbB-2* product. Jpn J Cancer Res. 1994;85:172–178.
18. Karpas A, Dremucheva A, Czepulkowski B. A human myeloma cell line suitable for the generation of human monoclonal antibodies. Proc Natl Acad Sci U S A. 2001;98:1799–1804.
19. Ishida T, Tsujisaki M, Hanzawa Y, et al. Significance of erbB-2 gene product as a target molecule for cancer therapy. Scand J Immunol. 1994;39:459–466.
20. Tam J. Synthetic peptide vaccine design: synthesis and properties of a high-density multiple antigenic peptide system. Proc Natl Acad Sci U S A. 1988;85:5409–5413.
21. Basak A, Boudreault A, Chen A, et al. Application of the multiple antigenic peptides (MAP) strategy to the production of prohormone convertases antibodies: synthesis, characterization and use of 8-branched immunogenic peptides. J Pept Sci. 1995;1:385–395.
22. Beselga J, Tripathy D, Mendelsohn J, et al. Phase II study of weekly intravenous Trastuzumab (Herceptin) in patients with Her2/neu-overexpressing metastatic breast cancer. Semin Oncol. 1999;26:78–83.
23. Hiramatsu H, Nishikomori R, Heike T, et al. Complete reconstitution of human lymphocytes from cord blood CD34+ cells using the NOD/SCID/gammacnull mice model. Blood. 2003;102:873–880.

Lentivirus vectors expressing short hairpin RNAs against the *U3*-overlapping region of HIV *nef* inhibit HIV replication and infectivity in primary macrophages

Takuya Yamamoto, Hiroyuki Miyoshi, Norio Yamamoto, Naoki Yamamoto, Jun-ichiro Inoue, and Yasuko Tsunetsugu-Yokota

Although successful attempts to inhibit HIV-1 replication in T cells using RNAi have been reported, the effect of HIV-specific RNAi on macrophages is not well known. Macrophages are key targets for anti–HIV-1 therapy because they are able to survive long after the initial infection with HIV and can spread the virus to T cells. In this study, we identified a putative RNAi target of HIV, consisting of the portion of the *nef* gene overlapping the U3 region (Nef366), and generated a lentivirus-based short hairpin RNA (shRNA) expression vector (Lenti shNef366). We show that Lenti shNef366 inhibits (1) HIV-1 replication in a monocytic cell line and in primary monocyte-derived macrophages (MDMs), (2) reactivation of latent HIV-1 infection, and (3) the production of secondary HIV-1 from MDMs harboring a genomic copy of Nef366. Moreover, we found that the up-regulated production of macrophage inflammatory protein 1β (MIP-1β), but not MIP-1α, in MDMs by Nef expression was considerably suppressed by Lenti shNef366, which suggests that HIV-1 dissemination to T cells through its interaction with HIV-1–infected MDMs can also be controlled by Lenti shNef366. Thus, lentivirus-mediated shRNA expression targeting the U3-overlapping region of HIV *nef* represents a feasible approach to genetic vaccine therapy for HIV-1. (Blood. 2006;108:3305-3312)

Introduction

HIV Nef, which is uniquely conserved among HIV-1, HIV-2, and SIV, is essential for viral replication in vivo.[1] Nef is located at the 3′ end of the viral genome, partially overlapping the 3′ long terminal repeat (LTR). The *nef* gene is one of the earliest expressed genes during HIV-1 replication and is transcribed at particularly high levels, often accounting for up to 80% of HIV-1–specific RNA in the early stages of viral replication. The Nef protein is multifunctional, having been shown to be involved in the down-regulation of CD4 receptor molecules, cell apoptosis, and signal transduction.[2-6] From studies of HIV-infected individuals, accumulating evidence indicates that Nef plays an important, albeit currently not clearly understood, role in the pathogenesis of AIDS.[1,2,6,7]

Recent investigations have shown that Nef has evolved macrophage-specific functions, such as the recruitment of T cells to sites of infection.[8] Macrophages expressing Nef secrete a high level of macrophage inflammatory protein 1α (MIP-1α) and MIP-1β, thus recruiting peripheral T cells to lymph nodes. More recently it was shown that Nef regulates the release of paracrine factors from macrophages[9]; at least 2 proteins have been identified, which enhance lymphocyte susceptibly to HIV-1 infection in the absence of cell-cycle progression. These results provide ample evidence that Nef functions as a virulence factor that contributes to the manifestation of the clinical symptoms of immunodeficiency. Thus, any therapeutic intervention aimed at either completely blocking or at least partially reducing the expression of *nef* during HIV infection would likely enhance the ability of the immune system to fight HIV infection.

Sequence-specific degradation of viral mRNA by the process of RNAi is a mechanism for selectively inhibiting the synthesis of viral proteins that are critical for HIV-1 replication. RNAi therapy is based on an existing mechanism of gene regulation that is ubiquitous in plants and animals, in which targeted mRNAs are degraded in a sequence-specific manner.[10] Quite recently, several groups reported the use of RNAi to successfully inhibit HIV-1 replication.[11-15]

To study the effect of stable expression of short hairpin RNA (shRNA) against the U3-overlapping region of HIV-1 *nef* on virus replication and Nef-mediated cytokine regulation in primary macrophages, we established a lentivirus vector system expressing HIV-specific shRNAs. We show that HIV replication in primary macrophages was considerably suppressed following transfection of shRNAs targeting the U3-overlapping region of genomic HIV *nef*. Moreover, RNAi was able to control CC-chemokine

From the Department of Immunology, National Institute of Infectious Diseases, Toyama, Shinjuku-ku, Tokyo; Subteam for Manipulation of Cell Fate, BioResource Center, RIKEN Tsukuba Institute, Tsukuba; Department of Molecular Virology, Bio-Response, Tokyo Medical and Dental University, Bunkyo-ku, Tokyo; AIDS Research Center, National Institute of Infectious Diseases, Shinjuku, Tokyo; and Division of Cellular and Molecular Biology, Department of Cancer Biology, Institute of Medical Science, University of Tokyo, Shirokane-dai, Minato-ku, Tokyo, Japan.

Submitted April 6, 2006; accepted June 29, 2006. Prepublished online as *Blood* First Edition Paper, July 20, 2006; DOI 10.1182/blood-2006-04-014829.

Supported by a grant from the Ministry of Health, Labor, and Welfare of Japan and from the Japan Health Sciences Foundation.

The authors declare no competing financial interests.

T.Y. and Y.T.-Y. performed laboratory experiments, data management, and the biostatistical analysis; T.Y., Naoki Y., J.-i.I., and Y.T.-Y. were responsible for the general design of the study; H.M. and Norio Y. were responsible for the design of the specific parts on lentivirus vectors and quantitative PCR analysis, respectively; T.Y., Y.T.-Y., and J.-i.I. were involved in the interpretation of the results and general outline of the paper; and T.Y. and Y.T.-Y. wrote the article.

Reprints: Yasuko Tsunetsugu-Yokota, Department of Immunology, National Institute of Infectious Diseases, Toyama 1-23-1, Shinjuku-ku, Tokyo 162-8640, Japan; e-mail: yyokota@nih.go.jp.

The publication costs of this article were defrayed in part by page charge payment. Therefore, and solely to indicate this fact, this article is hereby marked "advertisement" in accordance with 18 USC section 1734.

production associated with Nef expression in HIV-1–infected macrophages. Thus, lentivirus-vector–based RNAi of the *U3*-overlapping region of HIV-1 *nef* might have potential usefulness as a genetic vaccine against HIV-1 infection.

Materials and methods

Construction of plasmids

To express gene-specific shRNAs under the human U6-RNA promoter, sense and antisense oligonucleotides 47 bp in length were ligated into pENTR/U6 (Invitrogen, Carlsbad, CA). The sequences of the oligonucleotides were as follows: *lacz*, sense oligonucleotide, 5′-caccgctacacaaatcagcgatttcgaaaaatcgctgatttgtgtag-3′, and antisense oligonucleotide, 5′-aaaactacacaaatcagcgatttttcgaaatcgctgatttgtgtagc-3′; *Nef366* (nucleotides 366-385 of the HIV-1_{NL432} *nef* ORF overlapping the 3′ LTR), sense oligonucleotide, 5′-caccgattggcagaactacacaccaagagagtgtgtagttctgccaatc-3′, and antisense oligonucleotide, 5′-aaaagattggcagaactacacactctcttggtgtgtagttctgccaatc-3′. The resulting entry vectors were termed pENTR/shLacZ and pENTR/shNef366, respectively.

A Gateway-compatible (Invitrogen) HIV-1–based vector, pCS-RfA, containing elongation factor 1α promoter (EF-1α)–driven green fluorescent protein (EGFP) (pCS-RfA-EG),[16] was used to construct the lentivirus vectors, pCS-EG/shLacZ and pCS-EG/shNef366, according to the manufacturer's instructions (Invitrogen).

Cell culture and transfection

The human cell line 293T and human monocytic cell lines U937 and U1[17] were maintained in Dulbecco modified Eagle medium (DMEM) and RPMI 1640 medium (Gibco, Grand Island, NY), respectively, supplemented with 10% heat-inactivated fetal calf serum (FCS), penicillin (100 μg/mL), and streptomycin (100 μg/mL). To establish $CCR5^+$ CEMx174 cells expressing EGFP driven by HIV-LTR, CEMx174 cells were transfected with pEF-BOSbst-HuCCR5 and pHIV-1 LTR-EGFPpuro (kind gifts from M. Tatsumi, National Institute of Infectious Diseases, Tokyo, Japan) and CEMx174 CCR5/LTR-EGFP cells were established.

HeLa-CD4 cells (obtained from the National Institutes of Health AIDS Reagent Program) were transfected with pEF-Nef bst, and Nef-expressing HeLa-CD4 cells were established (HeLa-CD4-Nef).

RNAi target site selection

A Web-based program for designing siRNA targets (Promega, Madison, WI), BLOCK-iT RNAi Target Designer (Invitrogen), and the National Center for Biotechnology Information Web site were used for the selection of siRNA and shRNA sequences, and for BLAST searches. Stealth siRNAs were synthesized (Figure 1) and HeLa-CD4-Nef cells were transfected with 2.5 μL stealth siRNA complexed to 2.5 μL Lipofectamine 2000 (Invitrogen) according to the manufacturer's instructions. Total RNA was extracted and analyzed by quantitative reverse transcription–polymerase chain reaction (qRT-PCR) using specific LUX primers (Invitrogen) and the SuperScript III Platinum One-Step Quantitative RT-PCR system (Invitrogen). The sequences of the qRT-PCR primers were as follows: *nef* forward, labeled at its 3′ terminus with a reporter fluorophore 6-carboxyfluorescein (FAM), 5′-cagcagagtgtgattggatggcctgcFAMg-3′; *nef* reverse, 5′-tggctcagctcgtctcattctt-3′; *ef-1α* forward labeled at its 3′ terminus with a reporter fluorophore 6-carboxy-4′, 5′-dichloro-2′, 7′-dimethoxyfluorescein (JOE), 5′-gaaccacaagtgctaacatgccttggJOEtc-3′; *ef-1α* reverse, 5′-agcgtggttccactggcatt-3′. The reactions were performed using an Mx3000P (Stratagene, La Jolla, CA).

For Western blot analysis, cell lysates were prepared, subjected to 12.5% sodium dodecyl sulfate–polyacrylamide gel electrophoresis (SDS-PAGE), and immunoblotted with anti-Nef monoclonal antibody (mAb; F3, a kind gift from Dr Y. Fuji, Graduate School of Pharmaceutical Science, Nagoya City University, Nagoya, Japan). The blot was reacted with biotinylated goat anti–mouse IgG antibody (Jackson ImmunoResearch, West Grove, PA), then with streptavidin-POD (Roche, Indianapolis, IN).

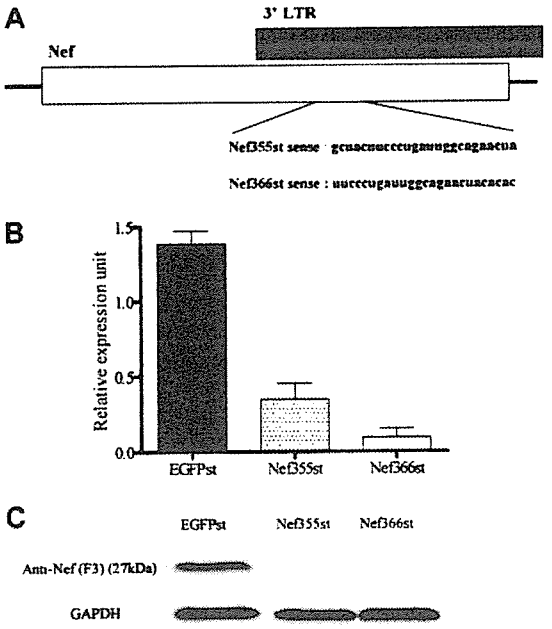

Figure 1. siRNA target sequences in *nef*. (A) Targets of siRNAs against the U3-overlapping region of HIV-1_{NL432} Nef and their sequences. Nef-expressing HeLa CD4 cells were transfected either with 2.5 μM *egfp* siRNAs (control: EGFPst) or *nef* siRNAs (Nef355st or Nef366st). At 48 hours after transfection, these cells were lysed to obtain total RNA and protein. (B) Total RNA was extracted and analyzed by qRT-PCR. The level of *nef* mRNA expression was normalized with that of elongation factor 1α (EF-1α) mRNA expression (*nef*/EF-1α). The data represent the expression level of *nef* mRNA relative to that of the control as 100%. The data represent the average ± SD of 3 independent experiments. (C) The cell lysates were subjected to 12.5% SDS-PAGE and immunoblotted with anti-Nef mAb.

Proteins were visualized by the SuperSignal Western Dura Extended Duration Substrate (Pierce, Rockford, IL) using an LAS3000 analyzer (Fuji Film, Tokyo, Japan).

Preparation of lentivirus vector

The lentivirus shRNA expression vectors were produced by transient transfection of 293T cells with a self-inactivating (SIN) vector construct, VSV-G– and Rev-expressing plasmid pCMV-VSV-G-RSV-Rev, and the packaging construct pCAG-HIVgp using the calcium phosphate precipitation method.[16] The lentiviral vector was concentrated by ultracentrifugation and the final solution was assayed for p24 antigen by an in-house enzyme-linked immunosorbent assay (ELISA).[18] The infectivity was determined by using 293T cells based on the EGFP expression.

Preparation of HIV-1 virus stocks

To prepare HIV-1, COS-7 cells were transfected with either pNL432, pNF462 (a kind gift from A. Adachi, Tokushima University, Tokushima, Japan), or pNF462dNef, in which the *nef* gene was deleted by digestion with *Xho*I and *Kpn*I, as described previously.[18]

Primary MDM culture

From peripheral blood mononuclear cells (PBMCs) of healthy, $HIV\text{-}1^-$ donors, $CD14^+$ monocytes were enriched using a magnetic-activated cell sorter (MACS; Miltenyi Biotec, Cologne, Germany) as described.[18] Monocytes were cultivated in RPMI 1640 medium supplemented with 10% FCS, 5% human AB plasma, and 10 ng/mL macrophage colony-stimulating factor (M-CSF) for 1 week to allow differentiation into monocyte-derived macrophages (MDMs).

Kinetics of virus production in stable shRNA-expressing U937 cells

Stable shRNA-expressing cells were infected with HIV-1_{NL432} for 2 hours, then cells were washed 5 times. Culture supernatants were harvested at 3- or

4-day intervals and viral production was monitored by HIV of p24 Gag antigen ELISA kit (RETRO TEC; ZeptoMetrix, Buffalo, NY).

Real-time RT-PCR (qRT-PCR) analysis of HIV-1 infection

HIV-1–infected cells were collected and total DNA was prepared 3, 8 and 12 hours after infection. For the detection and quantification of individual forms of HIV-1 DNA, oligonucleotide primer and probe sequences were designed specifically for the *Taq*Man assay as described elsewhere.[19] All probes (Biosearch Technologies, Novato, CA.) were 5′-labeled with the fluorophore FAM as the reporter dye, and 3′-labeled with Black Hole Quencher-1 (BHQ-1) as the quencher dye. The qRT-PCR analysis was performed on an Mx3000P (Stratagene) and the amount of HIV-1–specific DNA per cell was normalized to β-globin gene.

Kinetics of virus production in MDMs and reporter analysis

MDMs (2×10^5/well) were cultured in 48-well tissue-culture plates and infected either with wild-type HIV-1_{NF462} or HIV-$1_{NF462\Delta Nef}$. MDMs were infected with lentivirus at a multiplicity of infection (MOI) of 2 or 10 and washed extensively. The next day, cells were exposed to HIV-1 (5 ng/well) for 2 hours. Cell supernatants were harvested at 3- or 4-day intervals, and viral production was monitored by p24 antigen ELISA.

The cell-culture supernatants at 10 days after HIV infection were examined for infectivity, and 10 days after HIV infection, cell supernatants were collected (termed HIV-1/Lenti cont and HIV-1/Lenti shNef366). CEMx174 CCR5/LTR-EGFP cells were infected with HIV-1/Lenti cont or HIV-1/Lenti shNef366, and the number of HIV-1–infected EGFP$^+$ T cells was determined by fluorescence-activated cell sorter (FACS).

Detection of chemokines

For the detection of chemokine production in MDMs, the cytometric bead array (CBA) kit (BD Bioscience, San Jose, CA) was used, which measured 4 chemokines (IL-8, MIP-1α, MIP-1β, MCP-1) simultaneously.

Restimulation assay of lentivirus-transduced U1 cells

Latent HIV-1–infected U1 cells were transduced with Lenti cont or Lenti shNef366 at an MOI of 1. Two weeks later, EGFP$^+$ cells were sorted and stimulated with 1 ng/mL recombinant granulocyte-macrophage colony-stimulating factor (GM-CSF). Culture supernatants were collected at days 2 and 5, and the level of p24 antigen was measured by ELISA.

Results

siRNA suppresses *nef* mRNA and Nef protein expression

In the HIV-1 genome, *nef* is located at the 3′ end of the viral genome, partially overlapping the 3′ LTR (Figure 1A). Jacque and colleagues demonstrated previously that siRNA targeting of the 5′ region of *nef* (nucleotides 164-185) suppressed HIV replication.[20] Therefore, we selected 3 distinct regions of the HIV-1_{NL432} *nef* sequence using a Web-based program for designing DNA-directed RNAi systems, focusing on the Nef coding region overlapping the 3′ LTR. These were designated as Nef338, 366, and 479 based on the position of the first nucleotide of the siRNA. From initial screening experiments, we found that Nef366 was the most effective target site (data not shown).

The type 1 interferon response is an innate defense mechanism in eukaryote cells against viral infection. It has been shown that some types of siRNA induce type 1 interferon, which in turn mediates the gene-specific effect of RNAi.[21-23] The stealth siRNA system was developed to avoid the interferon response to siRNA in cells (Invitrogen manual). We prepared synthetic stealth siRNAs, designated Nef355st and Nef366st, and a control siRNA designated EGFPst, to determine the effect of RNAi using sequences based on Nef366 (the U3-overlapping region of the Nef-coding region). Neff355st was synthesized based on a Web-based computer program for generating stealth siRNA (Invitrogen), whereas Nef366st represents a slightly modified version of the stealth target site (6-nucleotide difference), so that it conformed to the target sequence as described. These stealth Nef siRNA sequences differed by only 5 nucleotides (Figure 1A).

We established a stable Nef-expressing HeLa-CD4 clonal cell line, designated as HeLa-CD4-Nef. HeLa-CD4-Nef cells were transfected either with 2.5 μM EGFPst or *nef* stealth siRNAs (Nef355st or Nef366st), and harvested 48 hours after transfection. Total RNA was extracted and the level of *nef* mRNA was measured by qRT-PCR. We observed that transfection with Nef366st reduced *nef* mRNA expression more than 90% (Figure 1B), whereas Nef355st suppressed the level of *nef* mRNA approximately 80%, compared with EGFPst controls. When cell lysates of the transfected cells were analyzed by Western blot, we found that both Nef366st and Nef355st suppressed Nef protein levels to below the detection limit of the assay (Figure 1C). Taken together, these results clearly showed that Nef366 is an efficient target sequence for the inhibition of *nef* gene expression by siRNA.

shRNA suppresses *nef* mRNA and Nef protein expression

To assess the effect of endogenous expression of Nef366 siRNA, we constructed expression vectors that encoded shRNAs corresponding to Nef366, or *lacZ* as a control, driven by the human U6 polymerase III promoter, designated as pENTR/shNef366 and pENTR/shLacZ, respectively (Figure 2A). HeLa-CD4-Nef cells were transfected with either pENTR/shNef366 or pENTR/shLacZ by FuGene6 reagent (Roche) and cells were harvested 72 hours after transfection. Total RNA was extracted and analyzed by qRT-PCR. We observed that the level of *nef* mRNA was suppressed by approximately 80% in cells transfected with pENTR/shNef366 (Figure 2B). Western blot analysis confirmed that pENTR/shNef366 strongly suppressed Nef protein levels as well (data not shown). These results indicated that promoter-driven endogenous

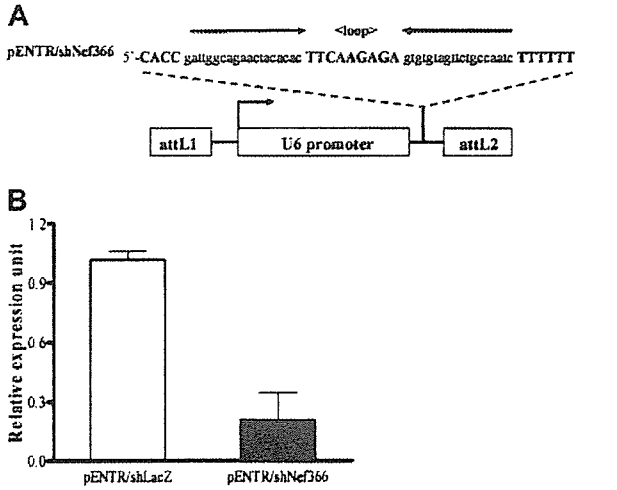

Figure 2. RNAi by transfection with shRNA expression vectors. (A) Schematic of the expression vectors (pENTR/shRNA) encoding shRNAs of Nef366 or *lacZ*, designated as pENTR/shNef366 and pENTR/shLacZ, respectively, in which expression is driven by the human U6 polymerase III promoter. (B) Nef-expressing HeLa-CD4 cells were transfected either with 1.0 μg pENTR/shNef366 or pENTR/shLacZ and cells were harvested 72 hours after transfection. Total RNA was extracted and analyzed by qRT-PCR. The data represent the average ± SD of 3 independent experiments.

expression of shNef366 was able to mediate RNAi of *nef* in HeLa-CD4-Nef cells.

Inhibition of HIV-1 replication in U937 cells by lentivirus-based shRNA expression

The transfection efficiency of the entry vectors used in suspension cells was quite low, and the objective here is to introduce siRNAs into primary macrophages. Therefore we constructed HIV-1–based lentivirus vectors expressing Nef366 shRNA or shRNA targeting lacZ as a control (Lenti shNef366 and Lenti control) using Gateway technology. The structure of the lentivirus vector used in the following studies is illustrated in Figure 3A.

To test whether Nef366 shRNA was able to efficiently block HIV-1 replication, we infected U937 cells with Lenti shNef366 or Lenti control, both of which encoded GFP driven by the EF-1α promoter (EGFP), at an MOI of 1. Two weeks after infection, nearly 30% of the cells stably expressed EGFP (Figure 3B upper panel). We sorted the EGFP$^+$ cells by fluorescence-activated cell sorter (FACSaria; BD Biosciences), after which the purity of the Lenti control– and Lenti shNef366–transfected, EGFP$^+$ cells was 97.2% and 99.7%, respectively (Figure 3B lower panel; U937/Lenti cont and U937/Lenti shNef366). The purified cell populations were then infected with 2 inoculation doses of HIV-1 (Figure 3C upper and lower panels; p24: 20 ng and 100 ng, respectively). The culture supernatants were collected at 3- or 4-day intervals, and the level of p24 antigen was measured by ELISA. We observed that at both inoculation doses HIV-1 replication in U937 cells was inhibited by Lenti shNef366, especially at the peak of HIV-1 production. The reverse transcriptase activity was also measured in parallel, and the result was consistent with that of p24 ELISA (data not shown). The inhibition of HIV-1 replication was sustained at least for 1 week, following which HIV-1 production gradually decreased in all cell populations, presumably because of the cytopathic effect of HIV-1 infection.

To further evaluate the effect of RNAi on the early steps of HIV-1 infection, we prepared cell lysates at different time points after inoculation (3, 8, and 12 hours after infection) and analyzed the level of reverse transcription activity by measuring the amount of different forms of proviral DNA (HIV-1 *2LTR* and *U5-Gag*) by the qRT-PCR. The copy number of these proviral DNA forms decreased in U937/Lenti shNef366 cells, relative to that seen in U937/Lenti control cells at all time points. The amount of these DNA forms normalized to β-globin gene at 12 hours after HIV-1 infection is depicted in Figure 3D. The copy number of *2LTR* and *U5-Gag* was 16.9% and 13.4% of control, respectively. These results suggested that the inhibition of HIV-1 replication occurred early after virus entry, presumably during uncoating or reverse transcription, not integration.

A type 1 interferon response has been shown to be induced by synthetic siRNAs via protein kinase R- (PKR) or toll-like receptor 7 (TLR 7)–mediated signaling pathways.[21-23] To eliminate the possibility that we were generating an interferon response following shRNA expression in our system, we analyzed the level of 2′ 5′-oligoadenylate synthetase mRNA expression in Lenti shNef366–infected U937 cells by qRT-PCR. We detected no such message (data not shown), indicating that the interferon response plays a

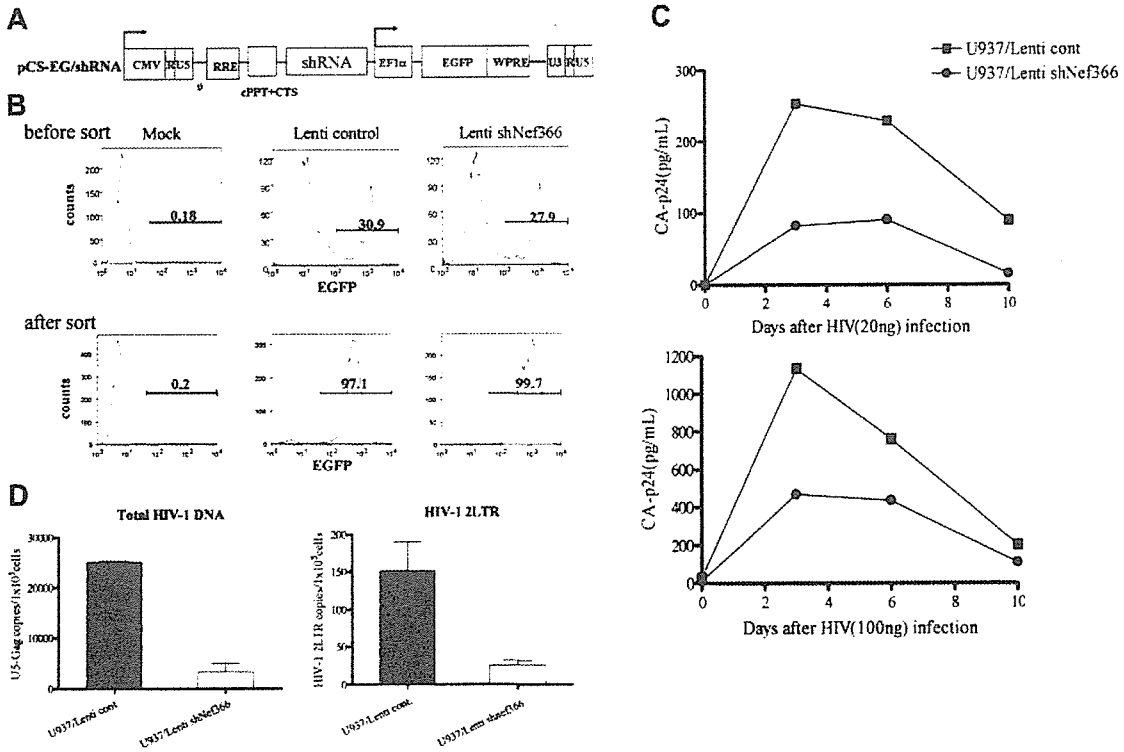

Figure 3. Inhibition of HIV-1 replication in U937 cells by lentivirus-mediated shRNA. (A) The structure of the shRNA lentiviral expression vector. The HIV-1–based lentivirus vector for expressing shRNA was constructed using Gateway technology. pCS-EG/shRNA consisted of U6-shRNA upstream of an EF1α promoter–driven EGFP expression cassette, which allowed simultaneous expression of shRNA and EGFP. (B) U937 cells were infected with lentivirus expressing either shNef366 (Lenti shNef366) or shLacZ (Lenti control) at an MOI of 1. After 2 hours of infection, cells were washed and maintained in culture. Cells expressing EGFP were analyzed by FACS, and EGFP$^+$ cells were collected. EGFP$^+$ cells were analyzed by FACSaria 1 week later (designated as U937/Lenti control and U937/Lenti shNef366). (C) U937/Lenti cont or U937/Lenti shNef366 cells (1×10^5/well) were infected with HIV-1_{NL432}, and the culture supernatants of these cells were collected at 3- or 4-day intervals after infection. The level of p24 antigen in the culture supernatants was measured by ELISA. (D) HIV-1–infected cells were collected and total DNA was prepared 12 hours after infection. Total HIV-1 and 2LTR DNA was analyzed by qRT-PCR. The amount of HIV-1–specific DNA per cell was normalized to β-globin gene expression. The data represent the average ± SD of 3 independent experiments.